Reference: *Biol. Bull.* **237:** 254–269. (December 2019)

DOI: 10.1086/705357

Foregut Development and Metamorphosis in a Pyramidellid Gastropod: Modularity and Constraint within a Complex Life Cycle

K. S. HARMS, A. V. HESKETH*, AND L. R. PAGE†

Department of Biology, University of Victoria, P.O. Box 1700, STN CSC Victoria, British Columbia V8W 2Y2, Canada

Abstract. Pyramidellids are tiny ectoparasitic gastropods with highly derived feeding structures for piercing and sucking. We attempted to resolve homology controversies about unique pyramidellid feeding structures by examining foregut development through larval and metamorphic stages, using sections for light and electron microscopy. We anticipated that, like many marine invertebrate larvae, post-metamorphic structures would differentiate extensively in late larvae to speed metamorphic transition. Previous studies of gastropods suggested that development of juvenile feeding structures in larvae was facilitated by foregut subdivision into dorsal and ventral developmental modules, and spatial uncoupling of these modules may have facilitated adaptive radiation in neogastropods. Observations of *Odostomia tenuisculpta* suggested that the stylet may be derived from cuticle-secreting buccal epithelium surrounding the proximal end of the salivary duct, whereas the stylet sheath could be either a derived jaw or a radular tooth. The anterior half of the remarkable buccal pump of these euthyneuran gastropods develops from the larval esophagus, which is unorthodox compared to caenogastropods, where extensive post-metamorphic specialization of a dorsal module component has not been previously described. The introvert tube develops from pouches of the distal larval esophagus and may actually be an eversible oral tube rather than an acrembolic proboscis. Minimal differentiation of presumptive juvenile foregut structures occurred during the larval stage of *O. tenuisculpta*, when compared to other gastropods. The stylet, stylet sheath, and buccal pump may be incompatible with functioning of the larval esophagus; thus, an explosive period of morphogenesis is necessary at metamorphosis. Although dorsal and ventral modules were recognizable during the development of *O. tenuisculpta*, we failed to find evidence that this modularity facilitated the extreme evolutionary remodeling of post-metamorphic feeding structures.

Introduction

Descent with modification has produced some extraordinary changes to ancestral morphology. The challenge of explaining large evolutionary changes involving functionally essential, multi-component complexes helped bring development back into conversations about evolution (Atchley and Hall, 1991; Raff, 1996; Wagner and Altenberg, 1996). From the beginning of these evo-devo conversations, a widely discussed concept has been developmental modularity (Raff, 2000; Schlosser and Wagner, 2004; Klingenberg, 2008; others reviewed by Esteve-Altava, 2017). A developmental module has been defined as a set of traits with pronounced internal interactions during development but weaker interactions with other modules (Wagner *et al.*, 2007; Klingenberg, 2008). Under the model of developmental modularity, phenotypic variants can arise within a developing module without fatally disrupting other modules of the complex, so new morphologies can be exposed to environmental selection (Raff, 1996; Hendrikse *et al.*, 2007).

The modularity of a developing system acquires an extra layer of complexity when life cycles include a larval stage, because larvae and adults have stage-specific structures and functions. For marine gastropods, much of the larval body is the initial template for the eventual juvenile or adult body (Page, 2009), so developmental modules first expressed in larvae may undergo temporal transformations as the selective landscape changes during and after metamorphosis. Two broadly applicable selective factors acting on morphogenesis

Received 11 April 2019; Accepted 4 July 2019; Published online 22 November 2019.

* Present address: Department of Zoology, University of British Columbia, Vancouver, British Columbia V6T 1Z2, Canada.

† To whom correspondence should be addressed. Email: lpage@uvic.ca.

during complex life cycles of marine invertebrates have been identified. Hadfield and coworkers (Hadfield, 2000; Hadfield *et al.*, 2001) noted that post-metamorphic structures typically begin forming in larvae prior to settlement and full metamorphosis. To explain this, they proposed a "need for speed" hypothesis, stating that initial development of juvenile structures in larvae has resulted from strong selection to promote rapid functionalization of the juvenile within the benthic habitat. However, a potential conflict arises from a counteracting larval constraint. As noted by Fretter (1969) for marine gastropods with feeding larvae, development of juvenile structures within larvae can occur only to the extent that larval functions are not compromised. Selection acting on complex life cycles has therefore influenced the temporal transformations of developmental modules.

Previous research on the developing foregut of marine gastropods with a larval stage generated a hypothesis incorporating developmental modularity to help explain two outcomes of past evolution. These are (1) rapid completion of metamorphosis by gastropod larvae, which requires that much of the complex, multi-component, post-metamorphic feeding system develop in larvae without interfering with larval feeding on microalgae, and (2) the spectacular array of derived foregut structures among adult gastropods, particularly among predatory neogastropods. The hypothesis proposed that the gastropod foregut consists of dorsal and ventral modules that each exhibit unique transformations during the full life history (Page and Hookham, 2017). The dorsal module forms the larval esophagus, which is partially lost during metamorphosis, although a retained part helps form the dorsal food channel. The ventral module originates from stem cells embedded in the ventral wall of the larval esophagus. An anterior population of these cells proliferates, forms an out-pocketing from the larval esophagus, and eventually differentiates into all components of the post-metamorphic buccal mass (except the roof of the dorsal food channel), including the cuticle-lined buccal cavity and jaw, a ribbon of recurved radular teeth supported by a cartilaginous or muscular odontophore, and a pair of salivary glands (Fig. 1A). Additional structures develop from the ventral module in predatory neogastropods with a long pleurembolic proboscis (Fretter, 1969; Page, 2000, 2005). Provision for almost complete spatial separation of larval and post-metamorphic feeding structures during the larval stage, as facilitated by separate developmental modules, may have contributed to what has been called an "explosive radiation" of neogastropods during the Cretaceous (Ponder, 1973; Taylor *et al.*, 1980). Phenotypic variants arising in the ventral module during development could be tested directly by the selective environment of the benthic juvenile, without needing to first pass a test of compatibility with the functioning larval esophagus (Page and Hookham, 2017).

Pyramidellid gastropods present the opportunity to test the prediction that dorsal and ventral foregut modules facilitated radical foregut evolution within constraints of a feeding larval

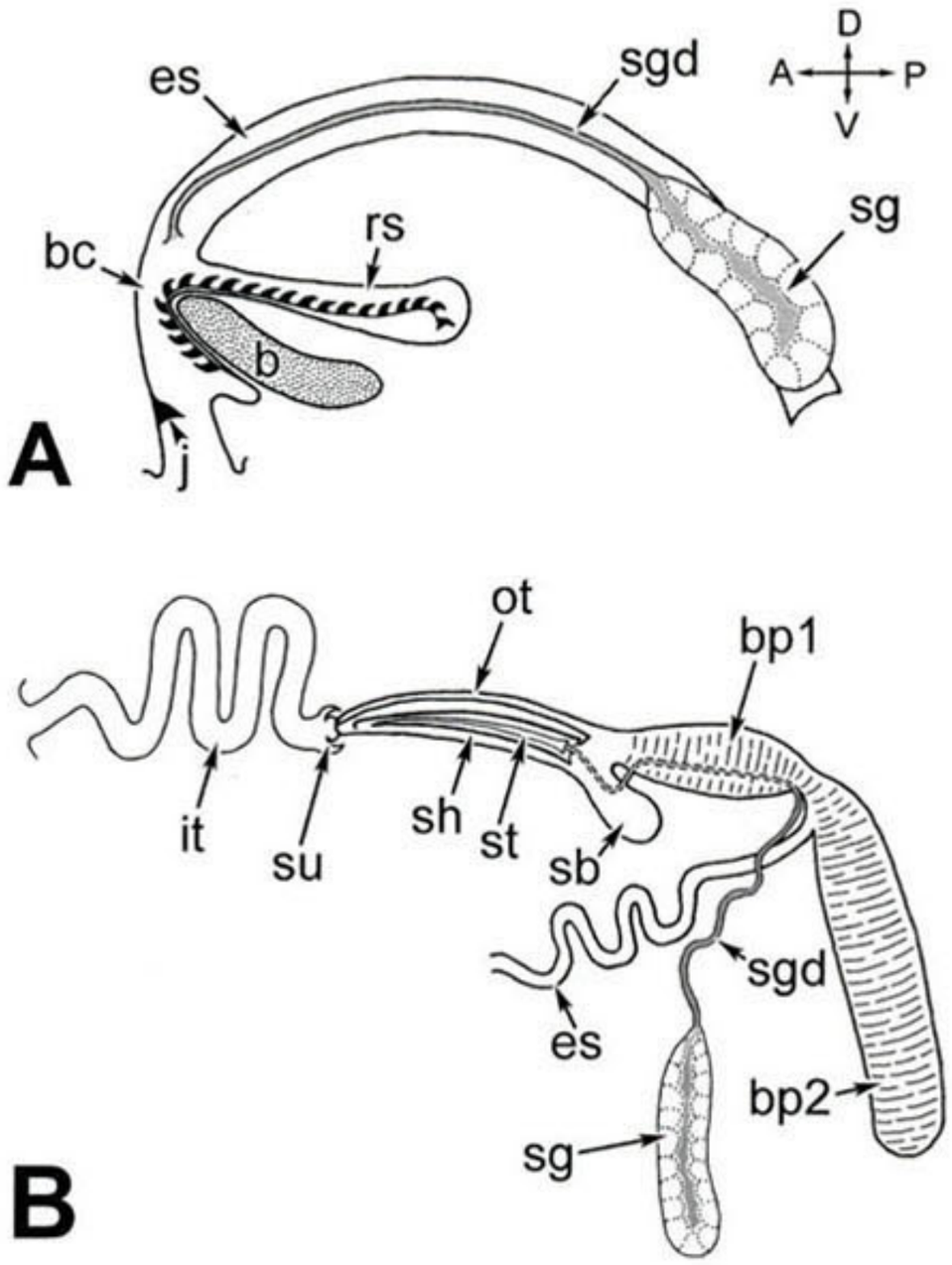

Figure 1. Sketches comparing adult foregut morphology of a herbivorous grazing euthyneuran gastropod, such as *Siphonaria denticulata* (A), with the highly derived adult foregut of a pyramidellid euthyneuran, such as *Odostomia tenuisculpta* (B). Images are not to the same scale; the right salivary gland and duct are not shown. b, radular bolster; bc, buccal cavity; bp1, buccal pump 1; bp2, buccal pump 2; es, esophagus; it, introvert tube; j, jaw; ot, oral tube; rs, radular sac secreting radula; sb, stylet bulb; sg, salivary gland; sgd, salivary gland duct; sh, stylet sheath; st, stylet; su, sucker. Orientation axes: A, anterior; D, dorsal; P, posterior; V, ventral.

stage. Pyramidellids are unusual euthyneuran gastropods because they feed with a proboscis, but they are phylogenetically distant from proboscis-bearing neogastropods (Dinapoli and Klussmann-Kolb, 2010; Zapata *et al.*, 2014). These tiny snails, some less than 3 mm in adult shell length (Schander *et al.*, 2003), feed on body fluids of much larger prey, usually annelids or other molluscs (Robertson and Mau-Lastovicka, 1979). Even when compared to the full array of spectacularly diverse and specialized gastropod feeding systems, the pyramidellid feeding system is remarkable (Fig. 1B). The pyramidellid proboscis is extended to the host and, in many but not all species (Schander *et al.*, 1999), attaches by a muscular sucker (Wise, 1996). The proboscis is described as acrembolic because it is extended by eversion and withdrawn by inversion (Fretter and Graham, 1949). A chitinous stylet, having the shape of a long, slender harpoon, is enveloped by a chitinous stylet sheath when not in use. During feeding, the stylet protrudes from an opening on the antero-ventral side of the stylet sheath and extends from the tip of the everted proboscis to puncture the host's body wall (Wise, 1993). Host body fluids are then

sucked into the foregut by a very large, typically two-part buccal pump (Ankel, 1949a, b; Maas, 1965; Wise, 1993, 1996; Hori and Okutani, 1995, 1996; Peterson, 1998; Schander *et al.*, 1999). The pyramidellid foregut is so derived that homologs of its various components are controversial. Ankel (1949a, b) interpreted the stylet as a highly modified radular tooth, whereas Fretter and Graham (1949) interpreted the stylet as a modified jaw because they placed it dorsal to the oral tube. However, Maas (1965) later showed that Fretter and Graham (1949) misinterpreted the dorsal and ventral sides of the pyramidellid foregut. Derivation of the muscular, cuticle-lined buccal pump is also uncertain, although Fretter and Graham (1949) suggested that at least the first half of the buccal pump (buccal pump 1) is part of the buccal cavity. Developmental data may help resolve homologs of both the stylet apparatus and the buccal pump (Maas, 1965), but previous descriptions of pyramidellid development did not include the foregut (White *et al.*, 1985; Cumming, 1993; Collin and Wise, 1997; Robertson, 2012).

We had two objectives for studying foregut development in the pyramidellid *Odostomia tenuisculpta* Carpenter, 1864, a species with a planktotrophic larva that lives along the Pacific Coast of North America (Abbott, 1974), where it feeds on a variety of molluscs (Harbo *et al.*, 2012; Maguire and Rogers-Bennett, 2013). First, by comparing results to developmental data for other gastropods, we hoped to establish homology between pyramidellid foregut components and foregut components of other gastropods. In particular, we compared foregut development during the larval phase of *O. tenuisculpta* to that of *Siphonaria denticulata*, which is another species of panpulmonate with a planktotrophic larva, described previously by Page *et al.* (2019). Second, we aimed to test the hypothesis that foregut developmental modularity has facilitated evolution of the highly derived post-metamorphic feeding system of *O. tenuisculpta*, despite a life history that begins with a feeding larval stage. Based on previous studies of caenogastropods, particularly proboscis-bearing neogastropods (Fretter, 1969; Page, 2000, 2005), we expected to find evidence that modular organization of the developing foregut has been important for facilitating advanced differentiation of post-metamorphic feeding structures within larvae, in a way that does not interfere with larval feeding.

Materials and Methods

To assist with understanding homology of foregut parts for *Odostomia tenuisculpta* Carpenter, 1864, we compared foregut development during the larval stage to that of another euthyneuran gastropod, the siphonarid *Siphonaria denticulata* Quoy & Gaimard, 1833. A description of overall larval and metamorphic development of *S. denticulata* and methods for culturing and processing the developmental stages for histological analysis have been previously given (Page *et al.*, 2019). Methods used for *O. tenuisculpta* are described below.

Source of adults and culture of larvae and juveniles

Adults of *O. tenuisculpta* were collected in July 2014 and May 2015 from the siphons of horse clams (*Tresus capax*) exposed at the sediment surface during low tide at Patricia Bay, southern Vancouver Island, Canada (48°26′21″N, 123°26′54″W). Collections were made under a scientific licence issued by the Department of Fisheries and Oceans Canada, Pacific Region. In the laboratory, adults were held in glass bowls containing 500 mL of seawater maintained at 12 °C; there they deposited fertilized eggs in gelatinous egg masses.

Hatched larvae were cultured at 12 °C in small glass bowls containing 100 mL of natural seawater passed through a prefilter by vacuum filtration. Initial density in culture was one larva per milliliter of seawater. To protect against heavy-metal contamination, the seawater was supplemented with ethylenediaminotetraacetic acid, disodium salt (EDTA) at a concentration of 8.6 nmol L^{-1}. Larvae were fed a mix of *Isochrysis galbana* and *Pavlova lutheri* (Bigelow National Center for Marine Algae and Microbiota, East Boothbay, ME; CCMP1323 and CCMP1325) that were cultured under continuous illumination in Provasoli's enriched seawater medium (Andersen *et al.*, 2005). Aliquots of microalgae were centrifuged, resuspended in pre-filtered seawater, and added to cultures to make a final concentration of 2×10^4 cells mL^{-1} during the first week of culture and 3×10^4 cells mL^{-1} thereafter. Density of microalgae was quantified with a hemacytometer. Streptomycin sulfate (Sigma, St. Louis, MO) was added at a concentration of 50 μg mL^{-1} (Switzer-Dunlap and Hadfield, 1977). Scant flakes of cetyl alcohol were sprinkled on the surface of cultures to reduce entrapment of the hydrophobic larval shells at the water-air interface (Hurst, 1967).

Larvae were transferred to fresh culture medium every one to two days. They were first concentrated by aspirating approximately half of the culture water, using a 10-mL syringe in which the syringe tip was cut off and replaced with Nitex (Genesee Scientific, San Diego, CA) cloth of 49-μm pore size. The concentrated larvae were transferred to a bowl of freshly prepared culture medium by hand-pipetting under a dissecting microscope.

Larvae were induced to metamorphose at or after 40 days post-hatch by transferring them to glass bowls containing prefiltered seawater and small pieces of periostracum stripped from a previously frozen siphon of *Tresus capax*. Juveniles were given small scallops (*Chlamys* spp.) as a food source.

Specimen preparation for thin and ultrathin sectioning

Larvae were fixed at five ages after hatching, and fixations were also performed at three time intervals after metamorphic loss of the velar lobes. Fixations of larvae were as follows, with number of specimens sectioned given in parentheses: newly hatched (5) and 10 (1), 20 (3), 30 (5), 40 (4), and 50 (3) days post-hatching. Metamorphs and juveniles were fixed at 1 (3), 4 (3), and 10 (2) days after loss of the velar lobes. Animals were anesthetized prior to fixation by using the two-step

procedure described by Page (2002). The primary fixative consisted of 2.5% glutaraldehyde in 0.2 mol L^{-1} phosphate buffer (pH 7.6) and 0.14 mol L^{-1} sodium chloride (Cloney and Florey, 1968). Specimens were stored in this fixative for up to 1 week at 6 °C. They were then decalcified in a 1:1 mixture of freshly prepared 10% EDTA and the glutaraldehyde fixative for about 2 hours at room temperature (Bonar and Hadfield, 1974). Decalcified specimens were rinsed 3 times in 2.5% sodium bicarbonate (pH 7.2) and post-fixed for 1 hour at room temperature in 2% osmium tetroxide in the bicarbonate buffer. After a brief rinse in distilled water, specimens were dehydrated in an acetone dilution series and embedded in Embed 812 (Electron Microscopy Sciences, Hatfield, PA) resin.

Sections for light microscopy were cut at a thickness of 0.8–1 μm, using a Diatome (Hatfield, PA) Histo Jumbo diamond knife and a Leica (Wetzlar, Germany) Ultracut UCT ultramicrotome. They were stained on a hot plate with a mix of methylene blue and azure II in sodium borate (Richardson *et al.*, 1960). Sections were photographed with a Zeiss (Oberkochen, Germany) Axioskop compound light microscope and an attached Retiga 2000R digital camera, using QCapture Pro 5.1 software (QImaging, Surrey, British Columbia, Canada). Brightness, contrast, and sharpness of images were adjusted using Adobe (San Jose, CA) Photoshop CS6.

Ultrathin sections for transmission electron microscopy were cut at 80–90-nm thickness by using a Diatome diamond knife. Sections were picked up on uncoated copper grids that had been briefly passed through a flame, and they were teased over spaces between the grid bars by using an eyelash tool. Sections were stained in a saturated aqueous solution of uranyl acetate for 60 minutes and rinsed; then they were stained in 0.2% lead citrate for 6 minutes and rinsed again. Ultrathin sections were examined with a JEOL (Peabody, MA) JEM 1011 transmission electron microscope.

Three-dimensional reconstructions

Surface-rendered 3-D reconstructions were prepared for a larva at 30 days after hatching and metamorphic stages at 1 and 4 days after velum loss. Serial sections for the larval stage were cut at 0.8-μm thickness through the entire foregut. Images of each section were placed in sequential order, and foregut profiles within each section were traced using a digitizing tablet and the Reconstruct software (ver. 1.1.0.0; Fiala, 2005). Resolution afforded by light microscopy was insufficient for distinguishing important details of morphology in metamorphic stages. Therefore, specimens at 1 and 4 days after velum loss were cut at a section thickness of 0.8 μm; but at intervals of 4–12 thick sections, 4 grids of thin sections were collected, representing about 2 μm of tissue thickness.

Results

Foregut development in the larva

Foregut development in larvae of *Odostomia tenuisculpta* is conveniently categorized into 3 stages: early (hatching and 10 days post-hatching), middle (20 days post-hatching), and late (30, 40, and 50 days post-hatching). No change in the foregut was noted between 40 and 50 days post-hatching. The entire larval digestive tract, including larval esophagus, stomach, left and right digestive gland, and intestine, was easily seen through the transparent shell of live larvae during the early stage of foregut development (Fig. 2A). Like other planktotrophic gastropod larvae, the larval esophagus had discoidal reticulate lamellae stacked between the microvilli and the cilia, arising from the epithelial cells (Fig. 2B). These lamellae are distinctive features of the velar food groove and larval esophagus of gastropod veligers, but they are absent from the post-metamorphic foregut (Bonar and Maugel, 1982). At hatching, the digestive tract of *O. tenuisculpta* was very much like that of

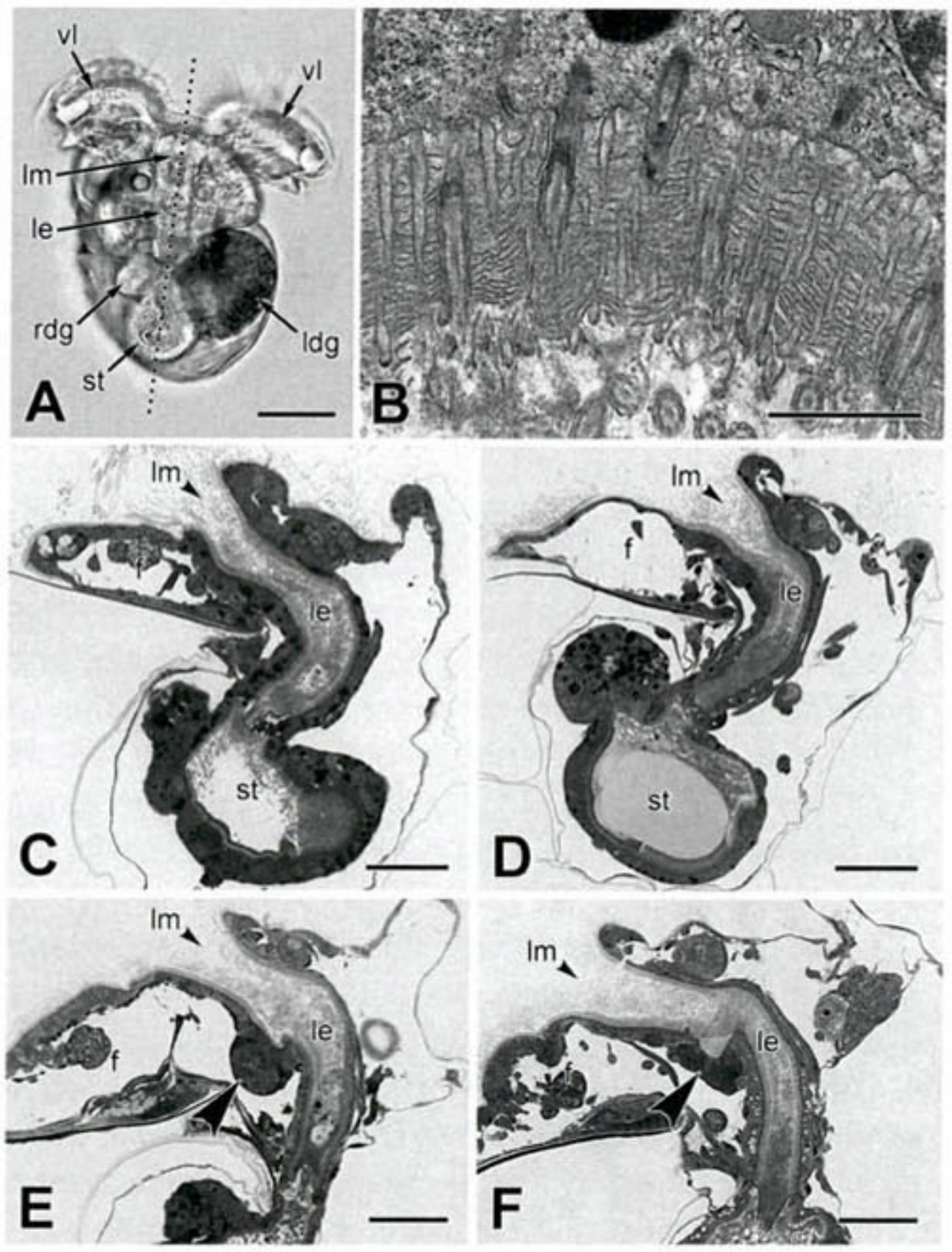

Figure 2. Early foregut development in the euthyneuran gastropods *Siphonaria denticulata* and *Odostomia tenuisculpta*. (A) Live early-stage larva of *O. tenuisculpta* (10 days post-hatching; ventral view) showing gut components; dotted line indicates section plane for (C–F). (B) Transmission electron micrograph (TEM) showing discoidal reticulate lamellae stacked between microvilli and cilia of the larval esophagus. (C) Mid-sagittal section through larval esophagus of *S. denticulata* at hatching. (D) Mid-sagittal section through larval esophagus of *O. tenuisculpta* at hatching. (E) Mid-sagittal section through larval esophagus of *S. denticulata* at middle stage of larval development; arrowhead indicates out-pocketing of hypertrophied epithelium. (F) Mid-sagittal section through larval esophagus of *O. tenuisculpta* at middle stage of larval development; arrowhead indicates out-pocketing of hypertrophied epithelium. f, foot; ldg, left digestive gland; le, larval esophagus; lm, larval mouth; rdg, right digestive gland; st, stomach; vl, velar lobe. Scale bars: (A), 50 μm; (B), 1 μm; (C–F), 25 μm.

newly hatched planktotrophic larvae of other euthyneuran gastropods, such as the siphonariid *Siphonaria denticulata*. In both species, the foregut at hatching consisted entirely of the larval esophagus, which was a simple, ciliated tube extending from the mouth to the stomach (Fig. 2C, D).

At the middle stage of obligatory larval development for both *S. denticulata* and *O. tenuisculpta*, histological sections showed the very early development of foregut structures that would become functional during feeding after metamorphosis. In *S. denticulata*, a patch of cells within the ventral wall of the larval esophagus had proliferated and enlarged and had formed an out-pocketing that bulged ventrally from the esophageal wall (Fig. 2E). This out-pocketing occurred at the point where the larval esophagus ran between the pair of statocysts. At the midpoint of larval development in *O. tenuisculpta*, we also saw an out-pocketing of hypertrophied cells within the ventral wall of the larval esophagus at the level of the statocysts (Fig. 2F).

After the middle stage of larval development, the foregut developmental pattern in *O. tenuisculpta* became markedly different from that in *S. denticulata*. When larvae of *S. denticulata* became capable of crawling (the pediveliger stage, when metamorphic competence was attained), the ventral out-pocketing of hypertrophied cells had differentiated into the cuticle-lined, post-metamorphic buccal cavity and radular sac (Fig. 3A, B). A ribbon of radular teeth emerged from the radular sac onto the floor of the buccal cavity; radular bolsters had differentiated beneath the ribbon of radular teeth; and salivary glands had differentiated, with ducts entering the dorsolateral walls of the presumptive post-metamorphic buccal cavity (Fig. 3B). The ciliated larval esophagus ran along the dorsal side of the structures for post-metamorphic feeding. At metamorphosis of *S. denticulata*, the distal larval esophagus between the mouth and the back of the buccal cavity completely dissociated (Page *et al.*, 2019).

By contrast, no evidence of stylet, stylet sheath, or buccal pumps was seen in late-stage larvae of *O. tenuisculpta*, nor was there a distinct partitioning of the ventral out-pocketing into areas of presumptive buccal cavity and radular sac. Instead, the ventral out-pocketing was somewhat funnel shaped, with its base extending as a very narrow channel that curved posteriorly (Fig. 3C). The columnar epithelial cells forming the wall of the ventral out-pocketing did not have cilia or discoidal reticulate lamellae at their apices. In addition, in late larvae of *O. tenuisculpta*, but not those of *S. denticulata*, a mass of cells accumulated over the lateral walls of the foregut in the area of the ventral out-pocketing (Fig. 3D).

The prospective post-metamorphic salivary glands were recognizable on either side of the larval esophagus in late-stage larvae of *O. tenuisculpta* (Fig. 4A, B), but the gland cells did not accumulate secretory product prior to metamorphosis. Ducts from the left and right salivary glands extended anteriorly, then swung ventrally before penetrating the posterior wall of the ventral out-pocketing, where the two ducts merged as a common salivary duct (Fig. 4A, C).

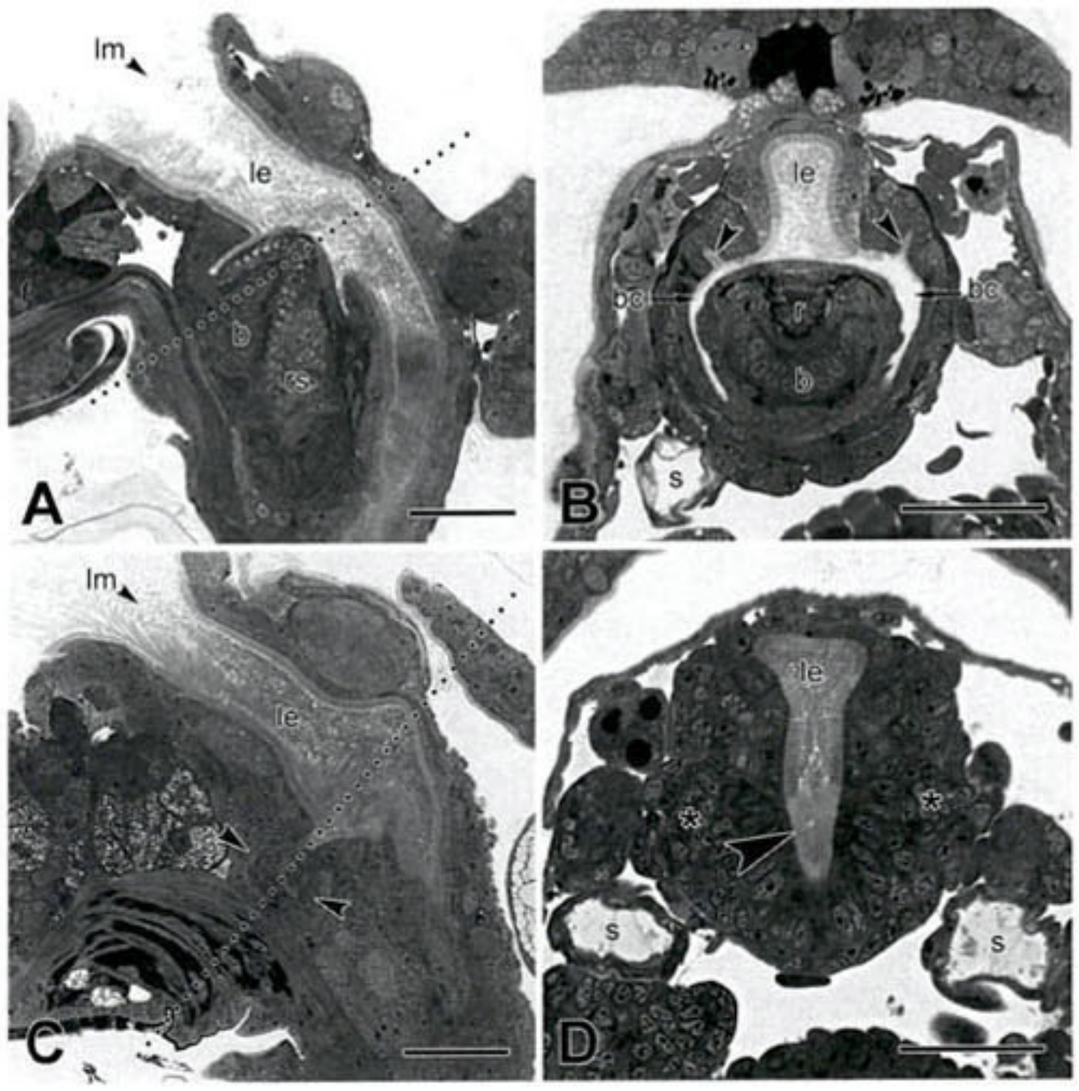

Figure 3. Histological sections through foregut of late larvae of *Siphonaria denticulata* and *Odostomia tenuisculpta*. (A) Mid-sagittal section of *S. denticulata* showing larval esophagus and extensive differentiation of post-metamorphic buccal mass; dotted line indicates section plane for (B). (B) Transverse section of *S. denticulata* passing through larval esophagus and presumptive post-metamorphic buccal mass; note ducts of salivary glands (arrowheads) entering cuticle-lined buccal cavity. (C) Mid-sagittal section of *O. tenuisculpta* showing larval esophagus and minimal differentiation of cells forming ventral out-pocketing (arrowheads); dotted line indicates section plane for (D). (D) Transverse section of *O. tenuisculpta* showing non-ciliated, columnar epithelial cells lining the ventral out-pocketing (arrowhead); asterisks indicate cells condensed over lateral walls of foregut. b, radular bolster; bc, buccal cavity; le, larval esophagus; lm, larval mouth; r, radula; rs, radular sac; s, statocyst. Scale bars: 25 μm.

Also during the last half of larval development in *O. tenuisculpta*, but not in *S. denticulata*, the ventro-lateral walls of the distal larval esophagus became embellished by a pair of conspicuous, elongate pouches that we call labial pouches (Fig. 5A, B). The pouches began just inside the larval mouth. Epithelial cells forming these pouches were distinct from other cells of the larval esophagus not only because of their large size and dense-packing, strongly staining cytoplasm but also because they were not ciliated; their apices gave rise to microvilli without discoidal reticulate lamellae (Fig. 5C).

Metamorphosis: one day after velum loss

Crawling larvae of *O. tenuisculpta* underwent metamorphosis in the presence of siphon periostracum from horse clams, with the first event being loss of the ciliated velar lobes. The most dramatic change to the foregut during the 24 hours after metamorphic loss of the velar lobes was complete loss of ciliated cells forming the distal larval esophagus. This ciliated tube was replaced by a tube of much smaller diameter (*cf.* reconstructions in Fig. 5A and 5D) and a laterally compressed lumen (*cf.* Fig. 5B and 5E). We call this the introvert tube.

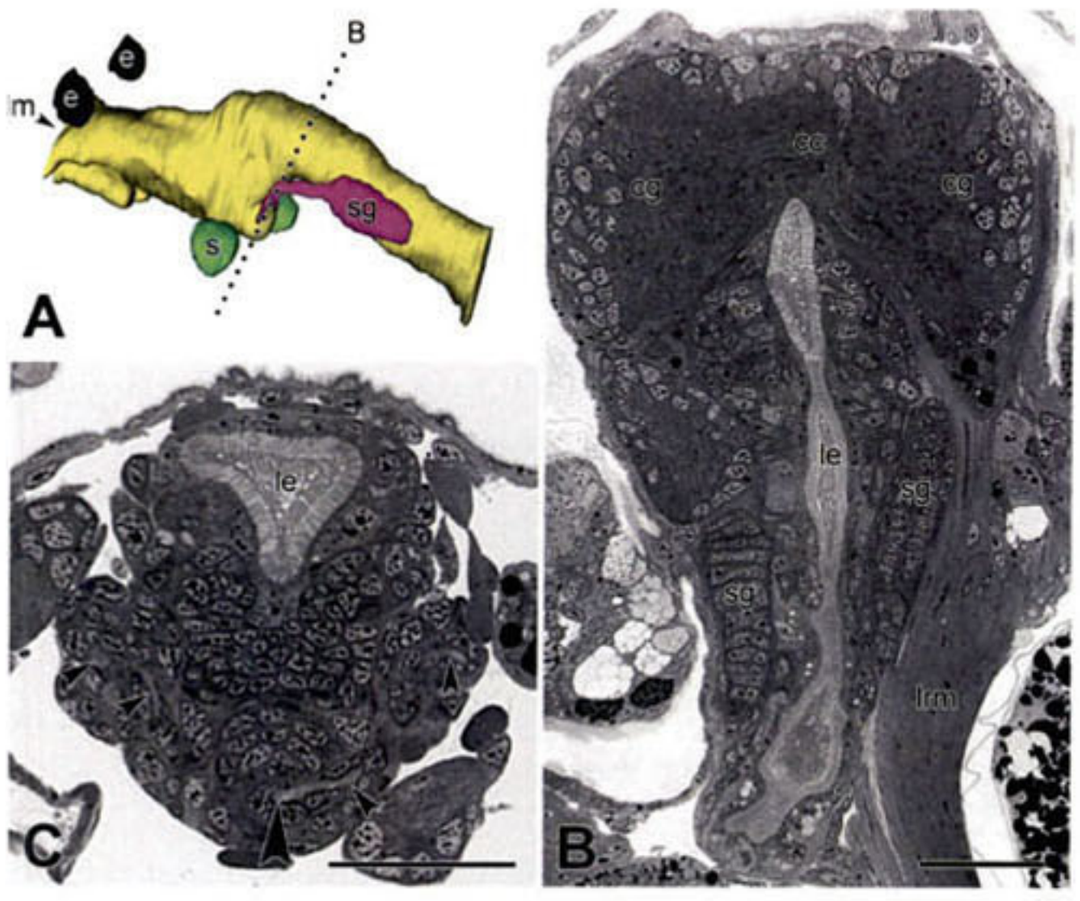

Figure 4. Salivary glands and ducts in late-stage larvae of *Odostomia tenuisculpta*. (A) Reconstruction of larval foregut in left lateral view of a late-stage larva showing ducts of salivary glands entering posterior end of ventral out-pocketing of foregut; dotted line indicates plane of section for (C). (B) Frontal section through foregut of late-stage larva showing salivary glands flanking larval esophagus. (C) Transverse section through posterior area of ventral out-pocketing in larva at 30 days post-hatching showing common salivary duct (large arrowhead) and multiple profiles through left and right salivary ducts (small arrowheads). cc, cerebral commissure; cg, cerebral ganglion; e, eye; le, larval esophagus; lm, larval mouth; lrm, larval retractor muscle; s, statocyst; sg, salivary gland. Scale bars: 25 μm.

Epithelial cells forming the introvert tube, like those of the labial pouches in the preceding larval stage, gave rise to microvilli but did not have cilia or discoidal reticulate lamellae (*cf.* Fig. 5C with 5E, inset, and 5F). Given the ultrastructural similarities between cells forming the labial pouches prior to metamorphosis and the introvert tube at one day after velum loss, we conclude that the labial pouches became the introvert tube. Presumably, as cells of the larval esophagus dissociated, the pouches opened up, their edges fused to form a closed tube, and the tube extended posteriorly to the level of the ventral out-pocketing. The external opening of the introvert tube replaced the larval mouth but was in the same position as the larval mouth.

The cross section through the introvert tube in Figure 5F passed through an isolated ciliated cell within the lumen. This was presumably a residual, dissociated cell of the larval esophagus in the process of being transported down the foregut to the digestive gland. Two more dissociated cells were seen within the foregut of this specimen, which was fixed at one day after velum loss. Sections of this and other specimens examined at one and four days after metamorphic loss of the velar lobes showed cells of the left digestive gland with large phagocytic vacuoles containing multiciliated cells, which we interpret as larval cells that had dissociated and been carried to the digestive gland during early metamorphosis.

To facilitate further description of foregut metamorphic changes in *O. tenuisculpta*, the sketches in Figure 6A–C summarize major changes to foregut regions between the late larval stage and one and four days after velum loss. The diagrams show the transformation of the labial pouches into the post-metamorphic introvert (blue shading) and indicate that the ventral out-pocketing from the larval esophagus is the presumptive buccal sac and stylet bulb (green shading) of the post-metamorphic animal. Data supporting these and other transformations shown in Figure 6 are provided in the following text and figures.

At one day after velum loss, the newly formed introvert tube arrived at the level of the ventral out-pocketing (presumptive buccal sac), as marked by the flanking statocysts (Fig. 7A, B). The ciliated larval esophagus was no longer present in this region. Instead, large cells that were conspicuous because of their large nucleus and prominent nucleolus bordered the lateral and ventral sides of a small lumen (Fig. 7B). Farther posteriorly from the large cells, the lumen of the presumptive buccal sac formed three deep channels (Fig. 7C).

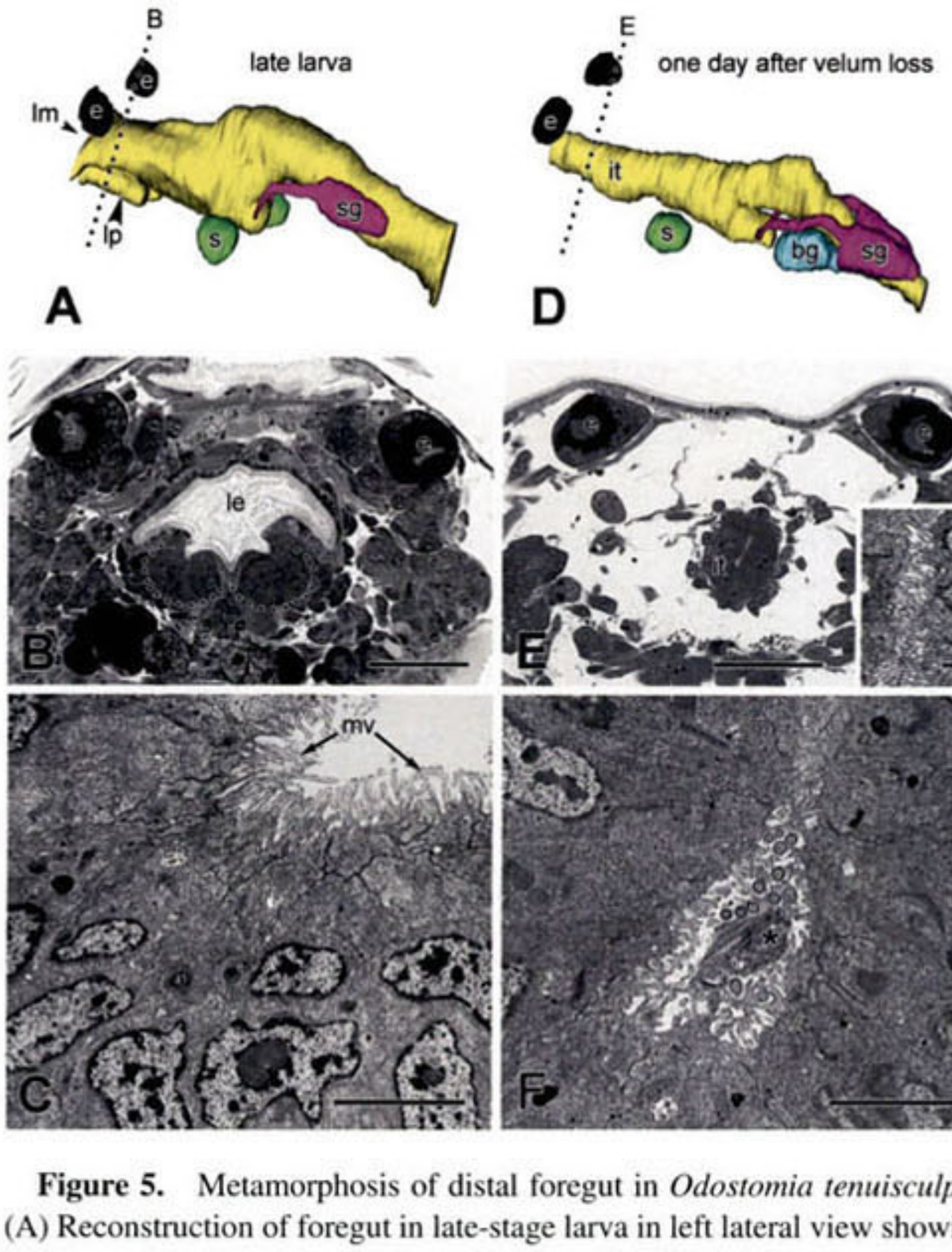

Figure 5. Metamorphosis of distal foregut in *Odostomia tenuisculpta*. (A) Reconstruction of foregut in late-stage larva in left lateral view showing labial pouches; dotted line is plane of section for (B). (B) Transverse section through distal larval esophagus; labial pouches outlined with dotted line. (C) Transmission electron micrograph (TEM) showing microvilli arising from cells of labial pouch. (D) Reconstruction of foregut at one day after velum loss; dotted line is plane of section for (E). (E) TEM showing distal foregut at one day after velum loss; ciliated larval esophagus replaced by much narrower introvert tube. (Inset) TEM of apical microvilli of introvert tube cells. (F) TEM showing disconnected ciliated cell (asterisk) within lumen of microvilli-lined introvert tube at one day after velum loss. bg, buccal ganglion; e, eye; it, introvert tube; le, larval esophagus; lm, larval mouth; lp, labial pouch; mv, microvilli; s, statocyst; sg, salivary gland. Scale bars: (B, E), 25 μm; (E inset), 0.5 μm; (C, F), 2 μm.

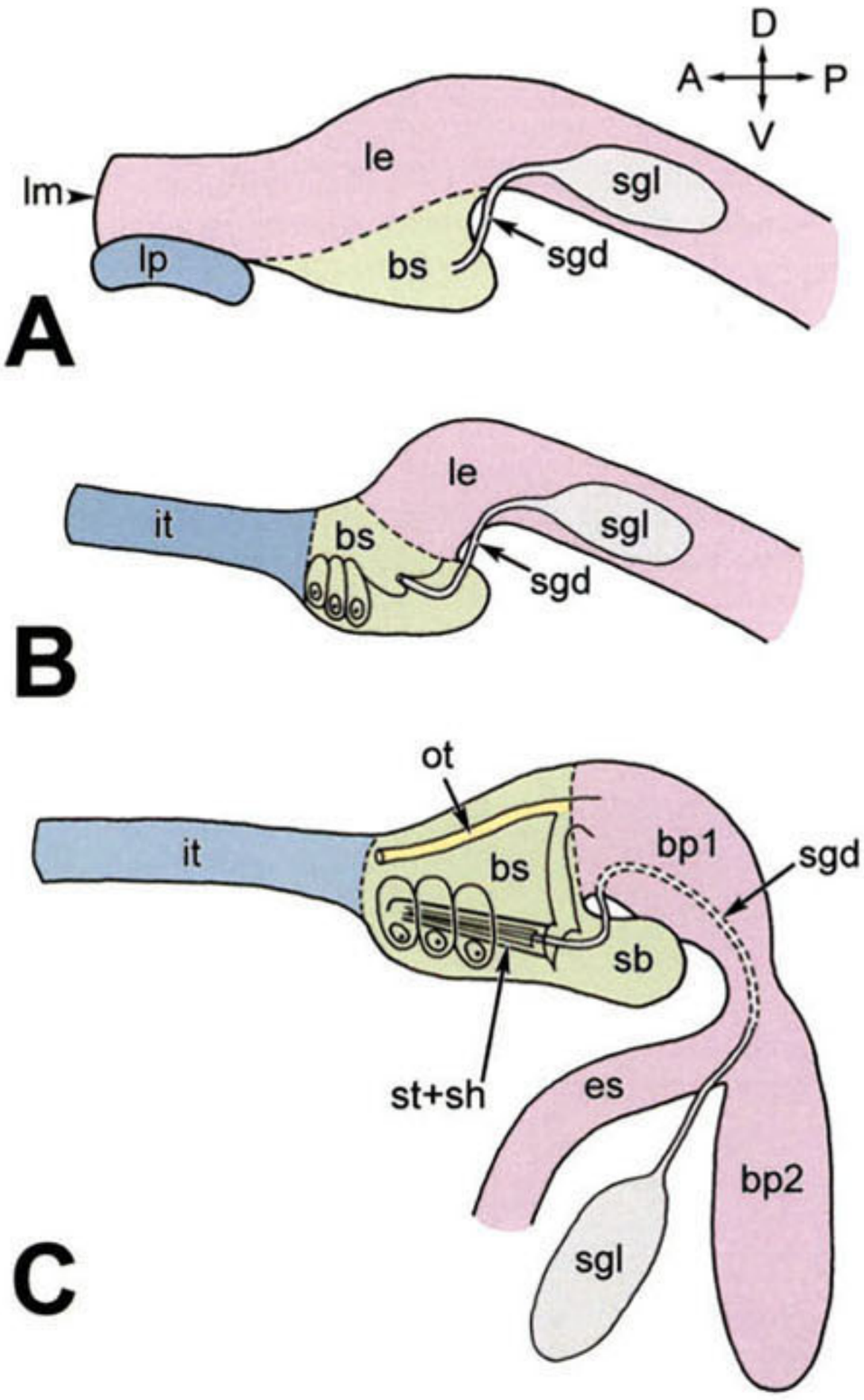

Figure 6. Sketches showing major events of foregut remodeling during metamorphosis of *Odostomia tenuisculpta*. All stages are shown in left lateral view; right salivary gland and its duct are not shown. Equivalent foregut areas are color coded: blue indicates labial pouch or introvert tube; pink indicates larval esophagus and post-metamorphic foregut regions derived from larval esophagus; green indicates presumptive buccal sac; yellow indicates post-metamorphic oral tube. (A) Late-stage larva. (B) One day after loss of velum. (C) Four days after loss of velum. bp1, buccal pump 1; bp2, buccal pump 2; bs, buccal sac; es, esophagus; it, introvert tube; le, larval esophagus; lm, larval mouth; lp, labial pouch; ot, oral tube; sb, stylet bulb; sgd, salivary gland duct; sgl, salivary gland; st+sh, stylet and stylet sheath. Orientation axes: A, anterior; D, dorsal; P, posterior; V, ventral.

Epithelial cells lining the dorsal channel were devoid of cilia but had microvilli and stacks of discoidal reticulate lamellae between the microvilli (Fig. 7D), which indicated that the dorsal channel was a retained larval esophagus. Cells lining the two ventro-lateral channels had short, irregular microvilli but no discoidal reticulate lamellae. At this level of the foregut, the small common duct of the salivary glands, bordered by stubby microvilli, ran within a ridge of cells between the two ventro-lateral channels (Fig. 7C and inset).

The ventro-lateral channels eventually separated from the dorsal channel and collectively formed a single crescent-shaped channel that continued posteriorly as the presumptive stylet bulb, which eventually ended blindly (Fig. 8A, B). Within the posterior end of the stylet bulb, the common salivary gland duct split into left and right salivary ducts; and each made a sharp dorsal turn to extend along the ventro-lateral margins of the dorsal channel (Fig. 8C, D). Discoidal reticulate lamellae were still present within the lumen of the dorsal channel above the stylet bulb (Fig. 8E) and within the remainder of the retained larval esophagus that extended to the stomach. Between the area where the metamorphosing foregut displayed a three-channeled lumen to well beyond the point where the prospective stylet bulb diverged from the dorsal channel, conspicuous cell masses bordered the lateral epithelial walls of the dorsal channel (retained larval esophagus). These cell masses are indicated by asterisks in Figures 7C, 8B, and 8C. The cell masses were noted in the previous late-stage larva; but at one day after velum loss, they had still not differentiated.

In summary, at one day after velum loss the ciliated cells of the distal larval esophagus had dissociated and had been replaced by the introvert tube that formed from the labial pouches. The introvert tube ran into the prospective buccal sac, which had conspicuously large cells embedded along the ventro-lateral wall of its anterior end. The posterior region

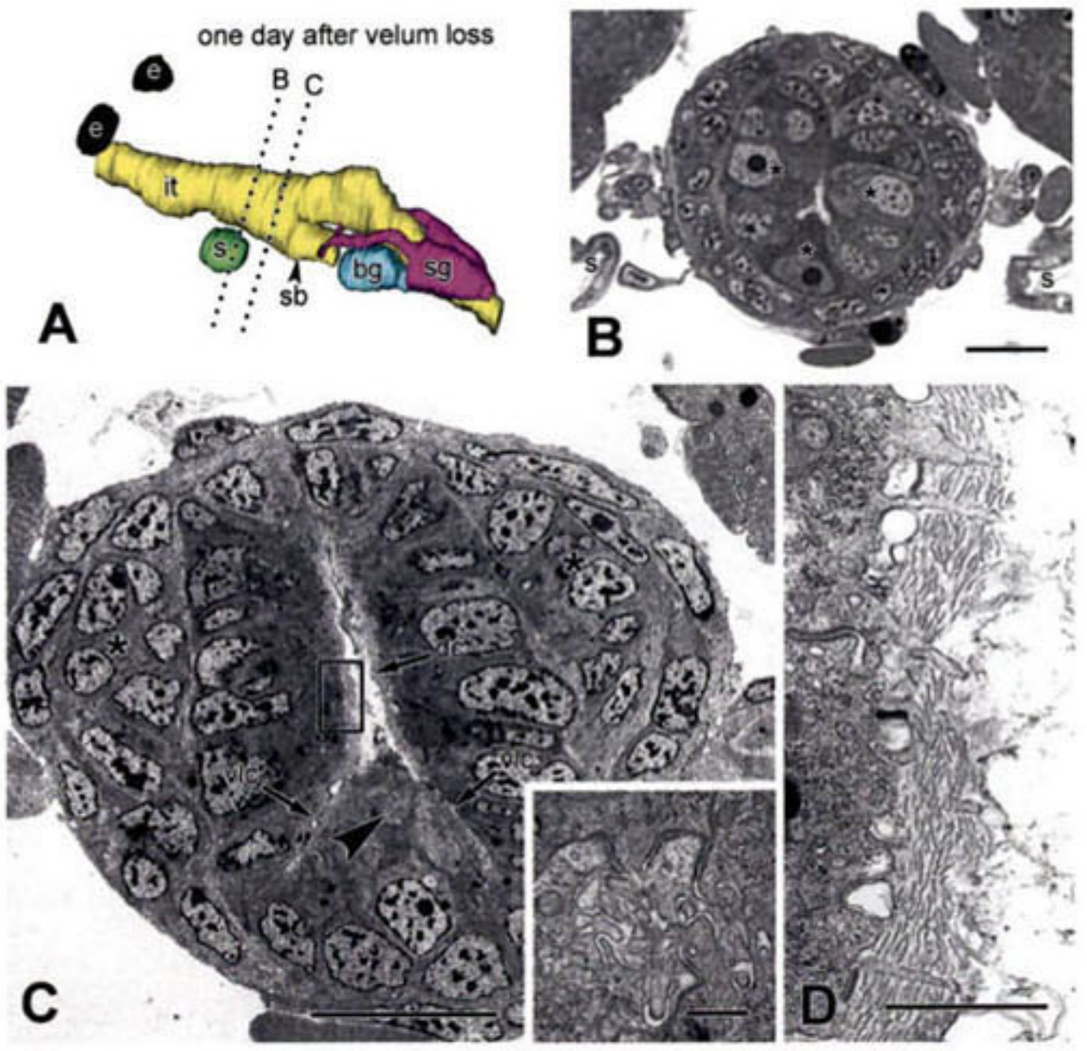

Figure 7. Future area of buccal sac of *Odostomia tenuisculpta* at one day after velum loss. (A) Reconstruction of foregut in left lateral view showing planes of section for (B) and (C). (B) Histological section through large cells (asterisks) bordering three-channeled lumen of foregut. (C) Transmission electron micrograph (TEM) through foregut immediately posterior to area of large cells; small arrows indicate three channels of lumen; large arrowhead indicates minute common duct of salivary gland (enlarged in inset); asterisks indicate accumulation of cells along lateral walls of foregut; boxed area of dorsal channel enlarged in (D). (Inset) Common duct of salivary gland. (D) TEM showing discoidal reticulate lamellae lining wall of dorsal channel. bg, buccal ganglion; dc, dorsal channel; e, eye; it, introvert tube; s, statocyst; sb, stylet bulb; sg, salivary gland; vlc, ventro-lateral channel. Scale bars: (B, C), 10 μm; (C inset), 0.5 μm; (D), 1 μm.

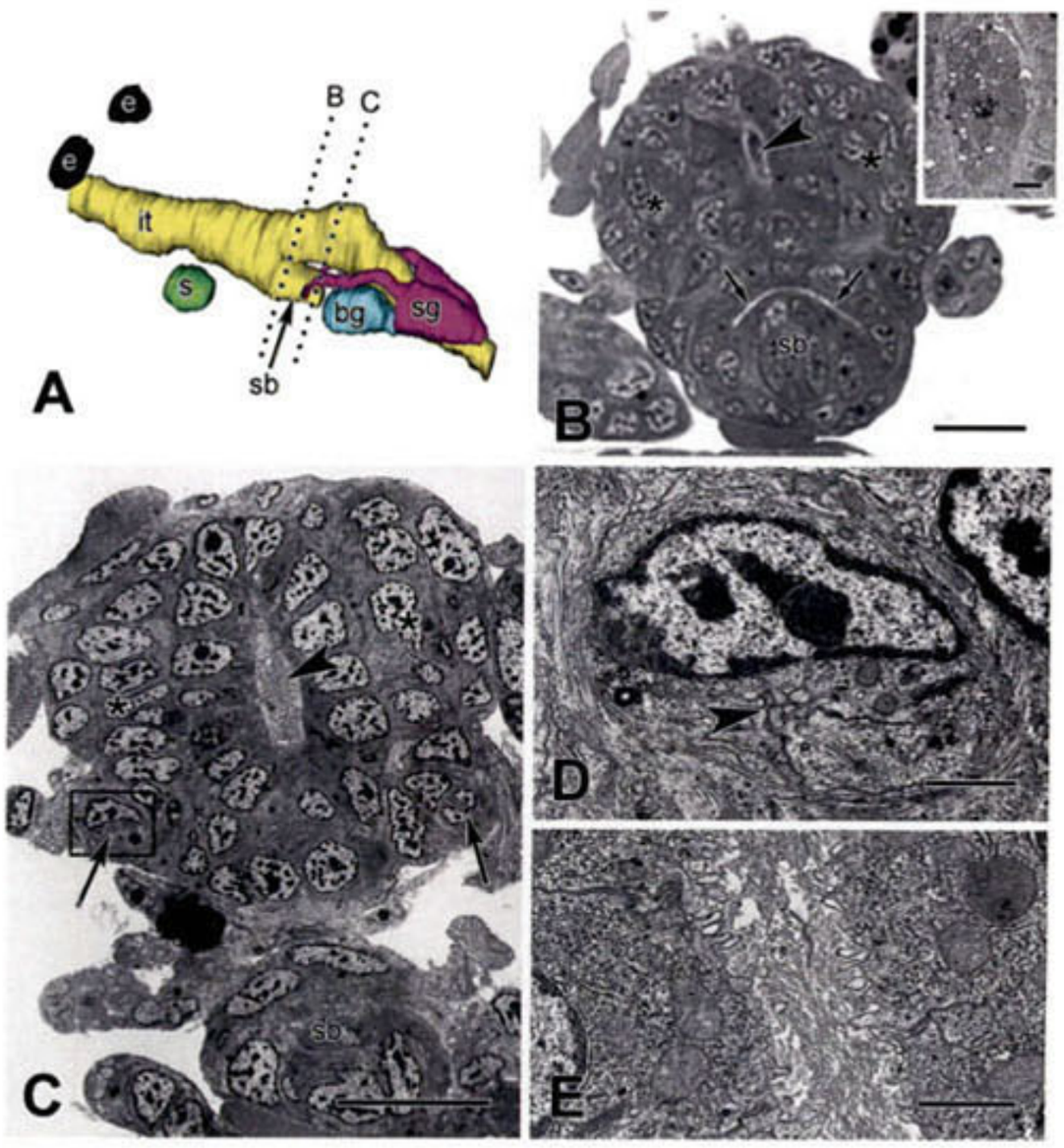

Figure 8. Developing buccal pump 1 and stylet bulb in *Odostomia tenuisculpta* at one day after velum loss. (A) Reconstruction of foregut in left lateral view at one day after velum loss; dotted lines indicate planes of section shown in (B) and (C). (B) Histological section showing stylet bulb and ventro-lateral channels (arrows) separated from dorsal channel (large arrowhead); a dissociated ciliated cell lies within dorsal channel (see inset); asterisks indicate cell masses adjacent to wall of dorsal channel. (Inset) Transmission electron micrograph (TEM) through dorsal channel showing dissociated ciliated cell within the lumen. (C) TEM through dorsal channel (arrowhead) and posterior extremity of the stylet bulb; asterisks indicate cell masses adjacent to dorsal channel; arrows indicate ducts of salivary glands; left salivary duct from a neighboring section enlarged in (D). (D) Duct of left salivary gland from section adjacent to (C); tiny lumen indicated by arrowhead. (E) Discoidal reticulate lamellae within lumen of dorsal channel in area of prospective buccal pump 1. bg, buccal ganglion; e, eye; it, introvert tube; s, statocyst; sb, stylet bulb; sg, salivary gland. Scale bars: (B, C), 10 μm; (B inset, D, E), 1 μm.

of the buccal sac at this stage consisted of a dorsal channel formed by a retained larval esophagus and a ventral prominence in which the common salivary duct was embedded. Cell masses that clustered over the lateral walls of the foregut had not differentiated during the day after velum loss; but, as described below, these cells became the muscle layers of buccal pump 1. Neither the stylet nor the stylet sheath was seen in any specimens sectioned at one day after velum loss.

Metamorphosis: four days after velum loss

Initial secretion of the stylet and the stylet sheath was seen in specimens sectioned at four days after metamorphic loss of the velum (Fig. 9A–D). The stylet sheath was embraced by cytoplasm of about eight very large cells ("lateral giant cells") within the ventro-lateral walls of the presumptive buccal sac (Fig. 9C). The central cavity of the tubular stylet was filled with multiple elongate, cytoplasmic processes containing longitudinally aligned microtubules. The lumen of the common salivary duct, which was very small and lined by stubby microvilli, ran between the cytoplasmic processes within the stylet (Fig. 9D). The cytoplasmic processes within the stylet extended from non-giant cells within the developing stylet bulb.

There were two cavities within the anterior half of the buccal sac at four days after velum loss. Immediately dorsal to the lateral giant cells secreting the stylet sheath, there was a cavity with a much-flattened lumen and the shape of an inverted V in cross-sectional profile. This cavity, which we call the

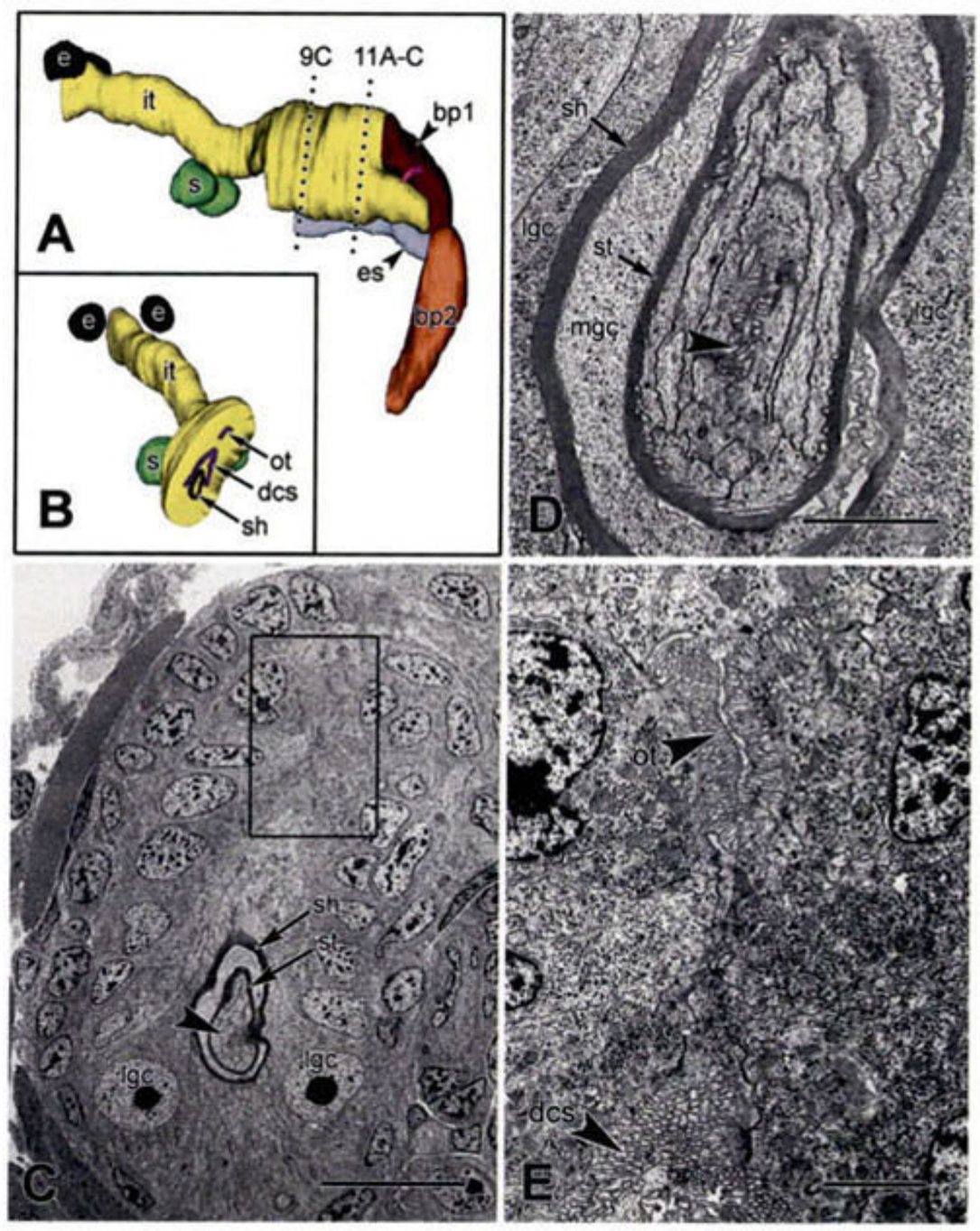

Figure 9. Anterior area of developing buccal sac of *Odostomia tenuisculpta* at four days after velum loss. (A) Reconstruction of foregut in left lateral view at four days after velum loss; dotted line indicates plane of section shown in (B) and (C). (B) Truncated reconstruction of foregut at four days after velum loss rotated to display plane of section shown in (C). (C) Transmission electron micrograph (TEM) showing initial stylet and stylet sheath; large arrowhead indicates common salivary duct within stylet that is enlarged in (D); boxed area enlarged in (E); note lateral giant cells. (D) TEM of stylet and stylet sheath; arrowhead indicates lumen of common salivary duct; note cytoplasm of medial giant cell between stylet and its sheath. (E) TEM showing newly formed oral tube and dorsal extremity of the dorsal cavity of the stylet complex (enlarged from C). bp1, buccal pump 1; bp2, buccal pump 2; dcs, dorsal cavity of stylet complex; e, eye; es, esophagus; it, introvert tube; lgc, lateral giant cell; mgc, medial giant cell; ot, oral tube; s, statocyst; sh, stylet sheath; st, stylet. Scale bars: (C), 10 μm; (D, E), 2 μm.

dorsal cavity of the stylet complex (dcs), is indicated in Figure 9B. It appears to correspond to what Maas (1965, p. 590, fig. 13b) called the *dorsale Höhlung um den Stachel*. The second cavity is the tiny microvilli-lined lumen of the forming oral tube of the post-metamorphic buccal sac (Fig. 9B, E). The dorsal cavity of the stylet complex ended blindly midway down the length of the stylet, whereas the oral tube continued posteriorly to merge with the lumen of the developing buccal pump 1 (described after further description of the stylet and the stylet sheath, given below).

Cuticle lining the buccal cavity of euthyneurans and other gastropods, including cuticle of the radula and jaws, is secreted by cells that extend microvilli into cuticle (*e.g.*, Wiesel and Peters, 1978; Hughes, 1979; Mackenstedt and Märkel, 1987; Mikhlina *et al.*, 2018). In metamorphosing larvae of *O. tenuisculpta*, cytoplasmic processes within the stylet extended sparse, short microvilli into the stylet cuticle down its entire length (Fig. 10A). However, the lateral giant cells associated with cuticle of the stylet sheath extended microvilli into the sheath cuticle only at its basal end, suggesting that the sheath grows from its base. The cytoplasm of lateral giant cells also included small electron-dense vesicles that may contain chitin precursor (Mikhlina *et al.*, 2018).

The stylet sheath embracing the stylet had a ventral opening at its extreme anterior end, and cytoplasm from a medial giant cell invaded this opening (Fig. 10B). Within the stylet sheath, cytoplasm of the medial giant cell covered the surface of cuticle forming both the stylet and the stylet sheath. Furthermore, where the medial giant cell invaded the sheath opening, its cell membrane was invaginated to form a network of irregular channels. Small electron-dense particles were seen within the channels, including areas where the channels bordered cuticle of the stylet and its sheath (Fig. 10C). Cytoplasm of the medial giant cell resided within the space between the stylet and its sheath along the anterior portion of the stylet complex (Fig. 9D), but it was absent along the basal area of the stylet complex (Fig. 10A). The medial giant cell and the multiple lateral giant cells were still recognizable at the base of the fully formed stylet in animals sectioned at 10 days after metamorphic velum loss (Fig. 10D).

Toward the posterior end of the buccal sac at four days after velum loss, the cuticular wall of both the stylet and the stylet sheath opened up to form two semicircles of cuticle; the semicircle continuing from the base of the stylet was immediately below the more irregular semicircular profile continuing from cuticle of the stylet sheath (Fig. 11A). Moving posteriorly, the semicircle of cuticle continuing from the wall of the stylet sheath re-closed, and the closed profile shifted dorsally toward the tiny oral tube (Fig. 11B). Ultimately, the closed profile of cuticle continuing from the base of the stylet sheath merged with the lumen of the oral tube (Fig. 11C, D). Meanwhile, the open semicircle of cuticle that was continuous with stylet cuticle continued posteriorly to eventually become one side of the lumen of the stylet bulb before disappearing altogether. The section shown in Figure 11C passes through the common duct of the salivary gland (enlarged in Fig. 11E), where it emerged from the basal end of the stylet proper.

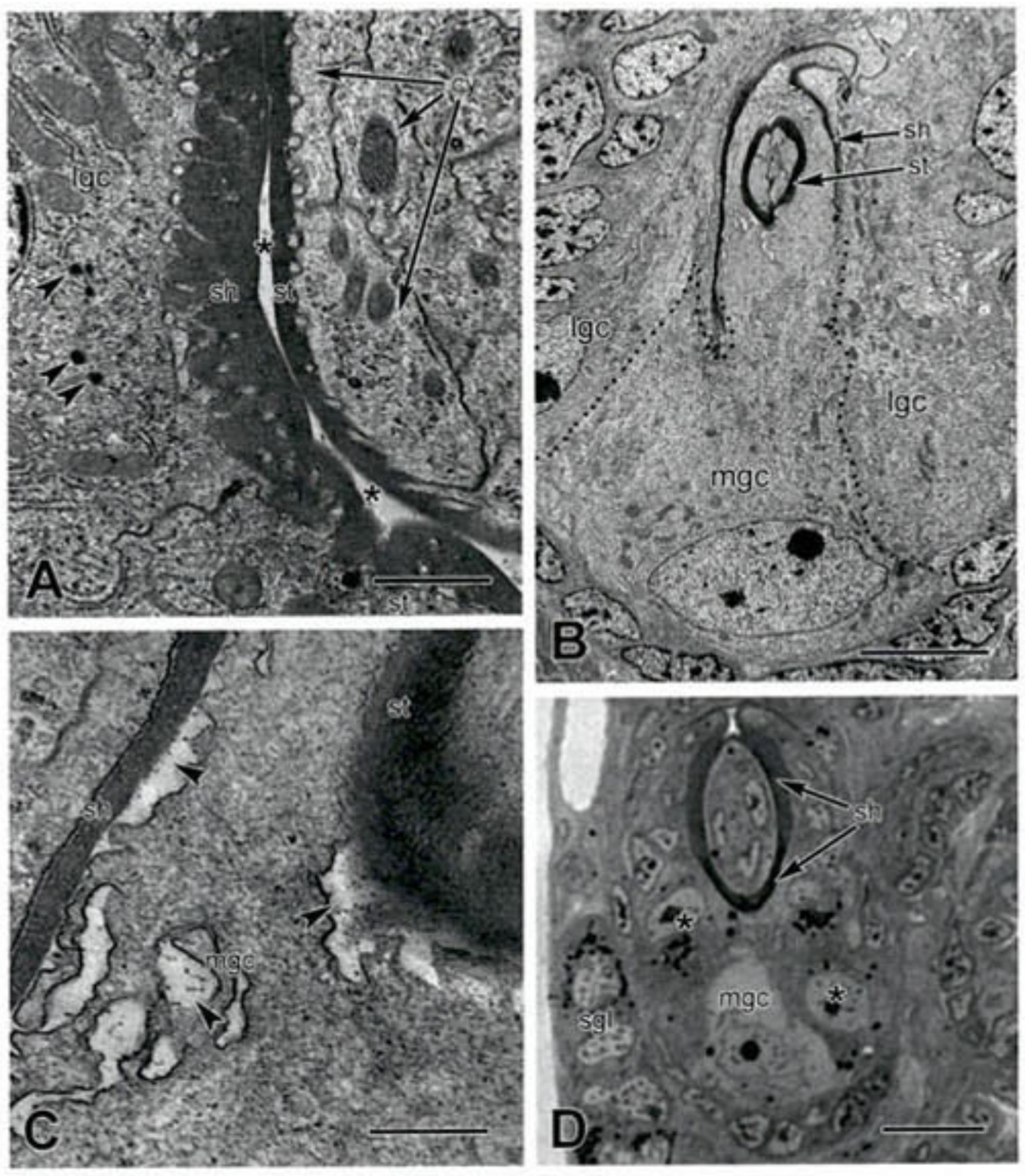

Figure 10. Stylet complex of *Odostomia tenuisculpta*. (A) Transmission electron micrograph (TEM) of transverse section through posterior area of stylet and stylet sheath at four days after velum loss; note microvilli from lateral giant cell penetrating into stylet sheath and microvilli from cytoplasmic extensions of salivary duct cells penetrating into stylet; arrowheads indicate electron-dense vesicles; asterisks indicate empty space between stylet and its sheath. (B) TEM of transverse section through apex of stylet complex showing cytoplasm of medial giant cell (partially outlined with dotted line) penetrating through opening in stylet sheath to cover cuticular surfaces of stylet and stylet sheath. (C) Membrane infoldings of medial giant cell (arrowheads) containing small electron-dense particles; also note fibrous nature of stylet cuticle. (D) Histological section through base of fully formed stylet sheath at 10 days after velum loss showing medial giant cell and 2 lateral giant cells (asterisks); nuclei within cells of adjacent salivary gland are also large. cy, cytoplasmic processes; lgc, lateral giant cell; mgc, medial giant cell; sgl, salivary gland; sh, stylet sheath; st, stylet; Scale bars: (A), 1 μm; (B), 5 μm; (C), 0.5 μm; (D), 10 μm.

Dorsal to the stylet bulb, the oral tube that had merged with the cuticle-lined compartment originating from the stylet sheath proceeded posteriorly as the lumen of buccal pump 1 (Fig. 12A, B). Discoidal reticulate lamellae were no longer present within the lumen of buccal pump 1, as they were at one day after velum loss. Instead, the lumen was lined by cuticle and had a triradiate profile (Fig. 12B).

The left and right salivary ducts, after diverging from the common duct and leaving the stylet bulb, immediately entered the cellular wall of buccal pump 1 (Fig. 12C, D). The section in Figure 12B shows profiles of the right salivary duct as it leaves the stylet bulb (enlarged in Fig. 12C) and also within

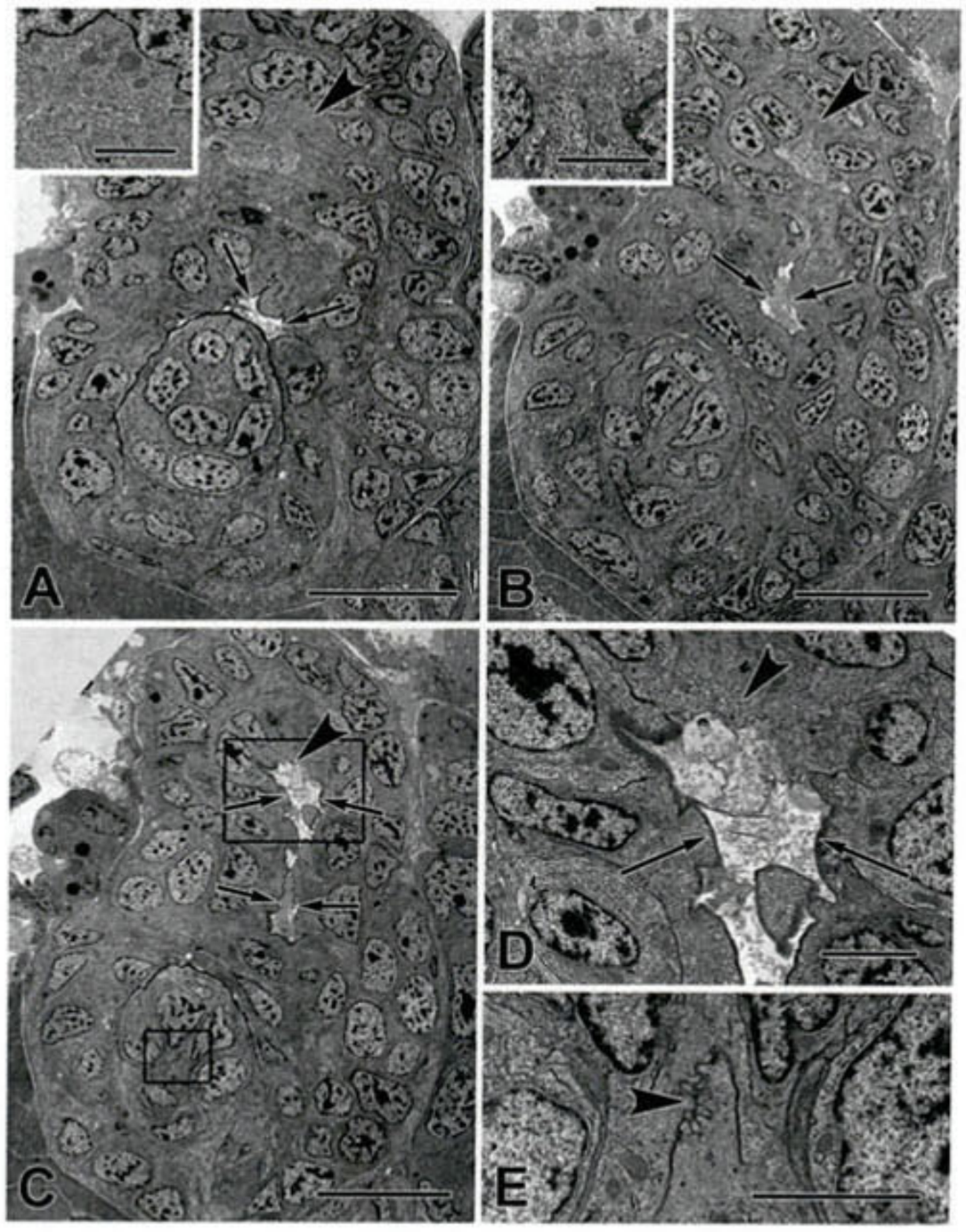

Figure 11. Posterior area of buccal sac of *Odostomia tenuisculpta* at four days after velum loss showing merger of cuticle-lined cavity from stylet complex with oral tube. (A) Transmission electron micrograph (TEM) of transverse section showing cuticle layer from stylet sheath (arrows) shifting dorsally from cuticle layer from stylet; large arrowhead indicates oral tube that is enlarged in inset. (Inset) Tiny microvilli-lined lumen of oral tube. (B) TEM showing cuticle-lined compartment (arrows) shifting farther dorsally; large arrowhead indicates lumen of oral tube enlarged in inset. (Inset) Tiny microvilli-lined lumen of oral tube. (C) TEM showing merger of cuticle-lined compartment (arrows) with lumen of oral tube (large arrowhead); boxed areas enlarged in (D) and (E). (D) Enlargement from (C) showing merger of cuticle-lined compartment (arrows) with microvilli-lined lumen of oral tube (large arrowhead). (E) Enlargement from (C) showing minute common salivary duct. Scale bars: (A–C), 10 μm; (D, E and insets of A, B), 2 μm.

the ventro-lateral wall of the presumptive buccal pump 1 (enlarged in Fig. 12D), because the duct angled slightly anteriorly after leaving the stylet bulb but then curved posteriorly after entering the wall of buccal pump 1.

Buccal pump 2 began to form at four days post-metamorphosis as a sausage-shaped body alongside the columellar muscle (Fig. 13A, B). The wall of buccal pump 2 was formed by epithelium secreting the cuticle that lined its lumen (Fig. 13C) and by multiple additional cell layers. Myofilaments had begun to differentiate within the most peripheral cells of the wall (Fig. 13D). The developmental origin of buccal pump 2 was not clearly observed. We assume that buccal pump 2 was built *de novo* from a subset of the cells congregated around the middle area of the foregut in late-stage larvae and at one day after velum loss.

At four days after velum loss, the esophagus emerged from the area between buccal pumps 1 and 2. Many cilia arose from the wall of the esophagus at this point of emergence (Fig. 13E and inset), but the remainder of the esophagus, as it traveled in a convoluted path to the much-reduced stomach, was mostly devoid of cilia. The terminal end of the stylet bulb contained a cresecent-shaped lumen lined by microvilli rather than cuticle (Fig. 13F).

Metamorphosis: 10 days after velum loss

Juveniles of *O. tenuisculpta* were first seen to extend the proboscis and feed on small scallops at 10 days after metamorphic velum loss. Histological sections through animals at 10 days after velum loss showed only 1 structure that was not recognizable at 4 days after velum loss: the muscular sucker

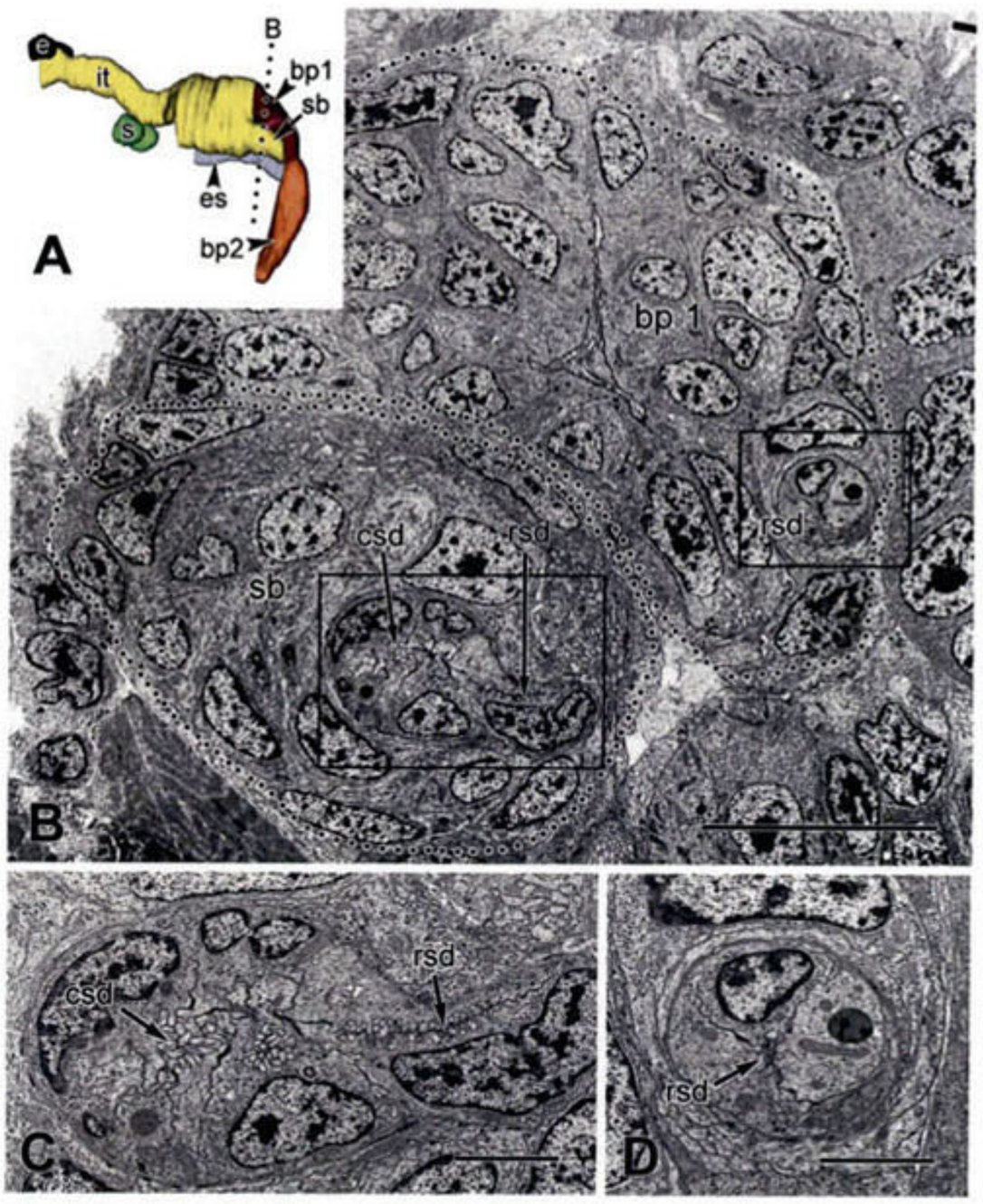

Figure 12. Presumptive stylet bulb and buccal pump 1 in *Odostomia tenuisculpta* at four days after velum loss. (A) Reconstruction of foregut in left lateral view at four days after velum loss; dotted line indicates plane of section shown in (B–D). (B) Transmission electron micrograph (TEM) passing through stylet bulb and cuticle-lined, triradiate lumen of buccal pump 1; note profiles of right salivary duct embedded in wall of buccal pump 1 and branching from the common salivary duct; boxed areas enlarged in (C) and (D). (C) Enlargement of right salivary duct branching from common salivary duct. (D) Enlargement of right salivary duct embedded in wall of buccal pump 1. bp1, buccal pump 1; bp2, buccal pump 2; csd, common salivary duct; e, eye; es, esophagus; it, introvert tube; rsd, right salivary duct; s, statocyst; sb, stylet bulb. Scale bars: (B), 10 μm; (C, D), 2 μm.

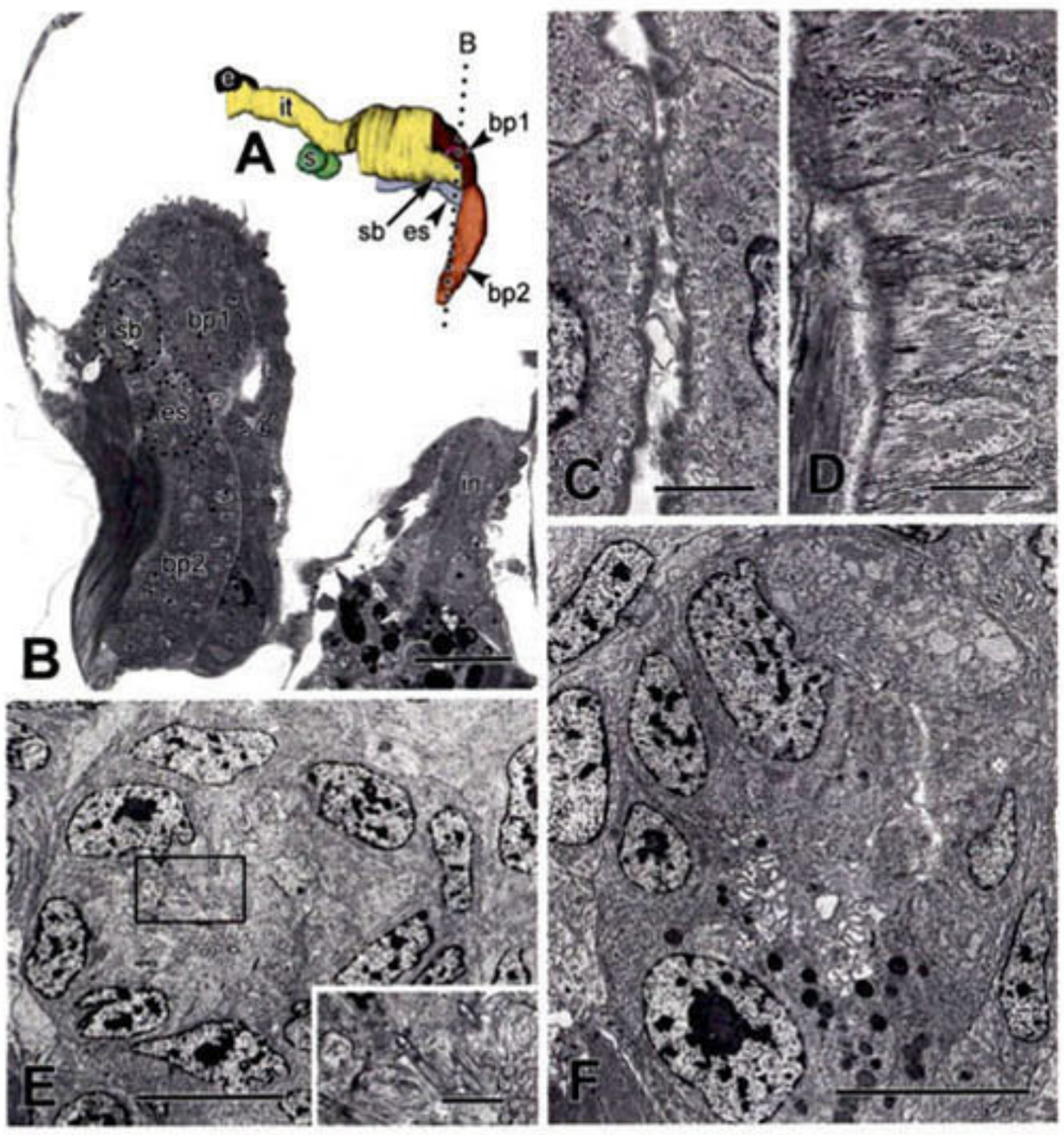

Figure 13. Buccal pumps, stylet bulb, and esophagus of *Odostomia tenuisculpta* at four days after velum loss. (A) Reconstruction of foregut in left lateral view at four days after velum loss; dotted line indicates plane of section shown in (B). (B) Histological section passing through buccal pumps 1 and 2, stylet bulb, and esophagus. (C) Cuticle lining lumen of buccal pump 2. (D) Transmission electron micrograph (TEM) showing myofilaments within peripheral cells of buccal pump 2. (E) TEM through esophagus where it leaves buccal pump 2; boxed area enlarged in inset. (Inset) Cilia arising from esophageal wall where it emerges from buccal bump 2. (F) TEM through posterior extremity of stylet bulb. bp1, buccal pump 1; bp2, buccal pump 2; e, eye; es, esophagus; in, intestine; it, introvert tube; s, statocyst; sb, stylet bulb. Scale bars: (B), 25 μm; (C, D, E inset), 1 μm; (E, F), 5 μm.

(Fig. 14A). In addition, between 4 and 10 days after velum loss the introvert tube had lengthened greatly; in retracted animals it formed several loops between the external opening on the head and the sucker. The stylet complex formed a long, curved dagger (Fig. 14B) measuring about 95 μm in length within an animal measuring only about 300 μm in shell length. The salivary glands were filled with secretory vesicles. As noted long ago by Ankel (1949a) for salivary glands of the pyramidellid *Odostomia plicata*, the nuclei of the salivary gland cells in *O. tenuisculpta* at 10 days post-metamorphosis were very large and elongate in shape (Fig. 14A, B).

Discussion

Homology of stylet and stylet sheath

Our observations on the developing stylet complex of *Odostomia tenuisculpta* suggest a hybrid structure, with the stylet and the sheath having different developmental and evolutionary derivations. However, the homology of the stylet sheath remains ambiguous, because it exhibited both jaw-like and radular tooth-like characteristics.

The stylet proper was secreted along long cytoplasmic processes extending from non-giant cells at the proximal end of the common salivary duct. At one day after velum loss, before stylet secretion had begun, the common salivary duct opened into the lumen of the buccal sac, the developmental homolog of the gastropod buccal cavity. The buccal cavity of euthyneuran gastropods, including *Siphonaria denticulata*, is lined by cuticle (Howells, 1942; Mackenstedt and Märkel, 1987; Mikhlina *et al.*, 2018); and ducts of the salivary glands discharge through the cuticularized wall of the buccal cavity. Therefore, we suggest that the stylet of *O. tenuisculpta* is best interpreted as an extension of buccal cuticle surrounding the entry point of the common salivary duct into the buccal cavity. Under this hypothesis, the stylet proper is a derived form of neither a jaw nor a radular tooth. As the stylet and contained salivary duct elongated during metamorphosis, they grew into the central cavity of the stylet sheath secreted by cells slightly more anterior within the buccal sac.

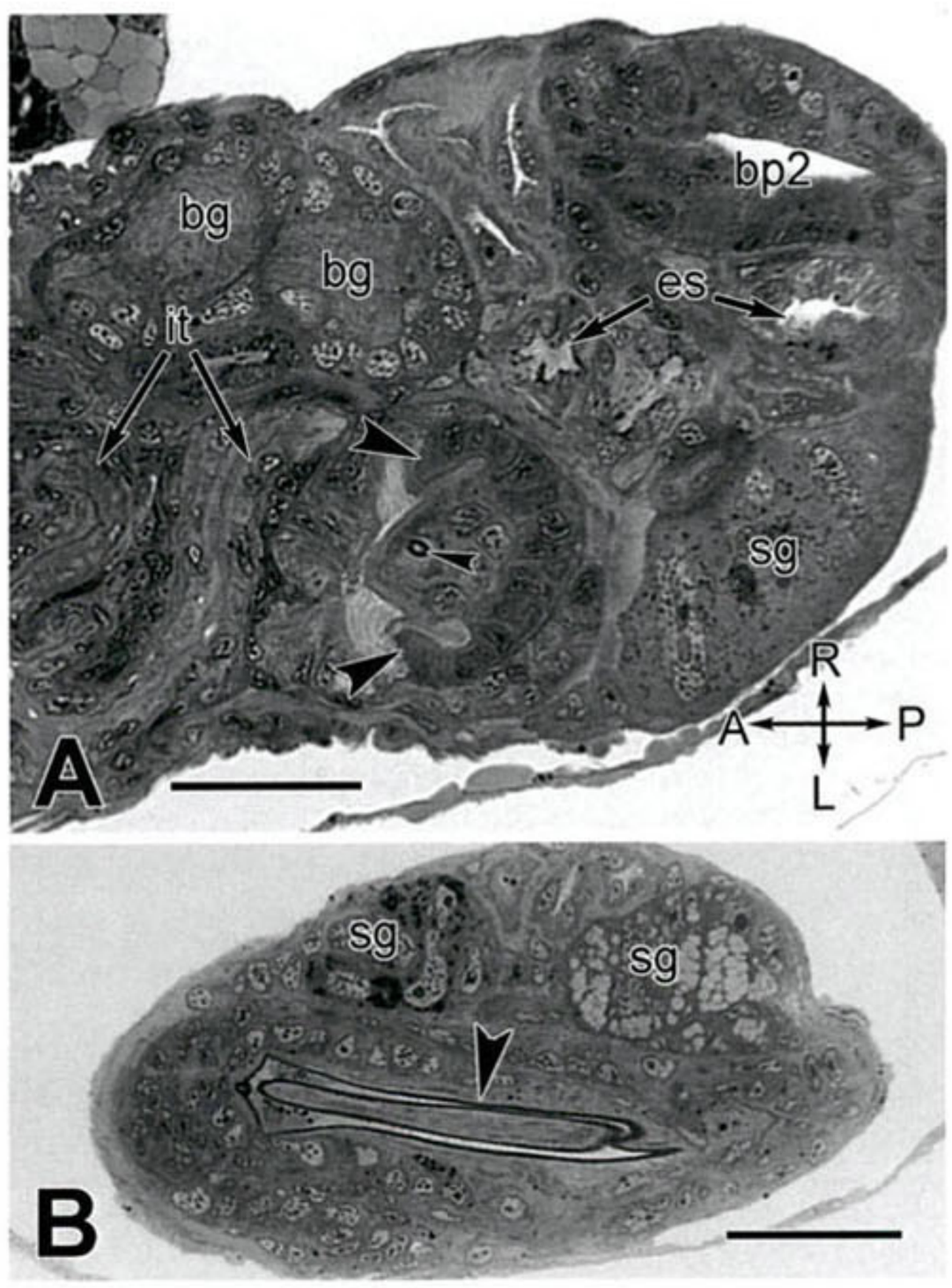

Figure 14. Foregut features of *Odostomia tenuisculpta* at 10 days after metamorphic velum loss. (A) Frontal section showing base of retracted introvert tube and rim of sucker (large arrowheads); small arrowhead indicates apical tip of stylet sheath within central tissue of sucker. (B) Tangential section through a portion of curved stylet and stylet sheath (arrowhead). bg, buccal ganglia; bp2, buccal pump 2; es, esophagus; it, introvert tube; sg, salivary gland. Orientation axes: A, anterior; D, dorsal; P, posterior; V, ventral. Scale bars: 25 μm.

The stylet sheath was less readily interpreted as an elaboration of previously non-specialized buccal cuticle. Unfortunately, however, a number of its characteristics were unhelpful for deciding between a jaw or radular tooth derivation, because the characteristics apply to both. The sheath was secreted over the microvillous apical surfaces of a cooperative group of cells within the ventral module. In other gastropods, both jaws and radular teeth are synthesized within the ventral module (Page and Pedersen, 1998; Page, 2002). Furthermore, although radular teeth are each molded by the three-dimensional shape created by the microvillous apical surfaces of a group of odontoblasts (Kerth and Krause, 1969; Runham, 1975; Mackenstedt and Märkel, 1987), a recent study has suggested the same process for shaping masticatory denticles of a nudibranch jaw by gnathoblasts (Mikhlina *et al.*, 2018).

Several characteristics of the stylet sheath of *O. tenuisculpta* were consistent with a jaw derivation. First, like jaws in two other gastropod species (Page and Pedersen, 1998; Page, 2002), the stylet sheath of *O. tenuisculpta* was secreted within the anterior portion of the ventral module. Second, like the jaw(s), but not radular teeth, in other gastropods, the stylet sheath is a non-iterative cuticular secretion maintained at a fixed position within the foregut. Finally, the wall of the stylet sheath was continuous with a cuticle-lined space that in turn continued into the cuticle-lined buccal pump 1, which is homologous with the initial part of the esophagus in other gastropods (see *Homology of the buccal pump*, below). This topology of parts suggests that the stylet sheath of *O. tenuisculpta* is a highly derived jaw.

Nevertheless, the stylet sheath also exhibited features that are reminiscent of radular tooth formation in other euthyneuran gastropods. Cells secreting the sheath are very large, with correspondingly large nuclei. Secretion of radular teeth by only a few very large odontoblasts that are probably polyploid is a distinctive feature of euthyneuran gastropods that has been described in nudibranchs (Hughes, 1979; Mikhlina *et al.*, 2018) and pulmonates (Kerth and Krause, 1969; Runham, 1975; Wiesel and Peters, 1978; Kerth, 1979; Mackenstedt and Märkel, 1987). However, if the unusual buccal hooks of the pteropod euthyneuran *Clione limacina* are truly jaw homologs, as suggested by Vortsepneva and Tzetlin (2014), then jaw-secreting gnathoblasts can also be very large. Possibly the strongest evidence in favor of a radular tooth ancestry for the stylet sheath comes from preliminary evidence for post-secretory modification of sheath cuticle. After the cuticle was secreted along the microvillous apical surface of lateral giant cells, the opposite surface of the sheath cuticle became invested by cytoplasm of a medial giant cell. Ultrastructural evidence suggests that the medial giant cell may add material to cuticle of both the sheath and the stylet proper, although this needs verification from additional research. Nevertheless, to date there is no evidence that jaw cuticle is modified after its secretion by cells on the superficial side of the cuticle, whereas many studies have shown that newly secreted radular teeth of molluscs are invested by cells of the superior epithelium of the radular sac (Wiesel and Peters, 1978; Hughes, 1979; Kerth, 1979; Mischor and Märkel, 1984; Mackenstedt and Märkel, 1987; Shaw *et al.*, 2009; Mikhlina *et al.*, 2018). These cells modify the chitinous matrix of the tooth cuticle by mineralizing or quinone tanning the chitin (Mackenstedt and Märkel, 1987 and additional references cited therein).

If the stylet sheath is indeed a highly derived radular tooth, then descent with modification has transformed a ribbon of consecutively secreted teeth that constantly moves anteriorly into a single tooth having a fixed position. If this surprising evolutionary transition actually occurred, then the anterior position of the stylet sheath and the giant "odontoblasts" that secrete it within the metamorphosing buccal sac is understandable, because a single tooth would need to be in a position where it can serve its function. The position of the stylet sheath (and its enclosed stylet) in pyramidellids is comparable to the position of the dagger-shaped "lead tooth" within the buccal mass of sacoglossan euthyneurans (see Hirose, 2005, fig. 4B), which puncture algal cells with a single row of often very elongate teeth (Jensen, 1993).

Introvert: acrembolic proboscis or eversible oral tube

Feeding tubes (various types of proboscides) that are temporarily extended during feeding are common among caenogastropods (Strong, 2003; Golding *et al.*, 2009; Simone, 2011), but they are unusual among euthyneuran gastropods. Nevertheless, members of the acteonoid genus *Hydatina* have an eversible oral tube (Rudman, 1972), and pyramidellids have a so-called acrembolic proboscis. In both of these euthyneuran groups, the feeding tube runs between an external opening on the head to the internal buccal cavity or sac, and it is everted during feeding. However, the two types of feeding tubes differ in how they form. In *Hydatina*, the tube is called an eversible oral tube because it presumably represents a great elongation of what is usually a very short chamber leading from the mouth into the buccal cavity of gastropods, the so-called buccal or oral tube (Fretter and Graham, 1962). Alternatively, the feeding tube in pyramidellids is called an acrembolic proboscis because the tube is presumably formed by invagination of a cylinder of head epidermis around the mouth, which carries the mouth deep into the cephalic hemocoel of the gastropod. If the feeding tube of pyramidellids is indeed an acrembolic proboscis, then the opening on the head of a non-feeding animal is not the true mouth (Fretter and Graham, 1949).

Our observations of the development of the eversible feeding tube of *O. tenuisculpta*, which we named the introvert tube, seemed inconsistent with its traditional interpretation as an acrembolic proboscis. The introvert tube formed from a pair of pouches from the ventro-lateral wall of the larval esophagus, immediately inside the larval mouth. If the introvert tube was truly an acrembolic proboscis, we would have expected an origin from cells outside the larval mouth.

Results of a developmental study of a species of moon snail, *Neverita* (=*Polinices*, =*Euspira*) *lewisii*, revealed that the acrembolic proboscis of this species developed very differently from the introvert tube of the pyramidellid *O. tenuisculpta*. Juveniles of *N. lewisii* fed for at least several weeks after metamorphosis before the acrembolic proboscis began to form. The very young juveniles had an accessory boring organ located well outside the mouth on the lower lip (Page and Pedersen, 1998). However, the accessory boring organ of adult moon snails lies at the tip of the acrembolic proboscis, demonstrating that the acrembolic proboscis of this species forms by inward growth of head tissue that was originally outside the mouth. The inward growth occurs slowly during postmetamorphic life. In *O. tenuisculpta*, by contrast, the eversible feeding tube was functional when animals took their first postmetamorphic meal, because it formed rapidly from labial pouches located just inside the larval mouth. It would be informative to compare development of the introvert tube in *O. tenuisculpta* to development of the long, eversible oral tube in a member of the genus *Hydatina*. At present, our ability to interpret ancestral derivation of the introvert tube of *O. tenuisculpta* is compromised by the fact that very little information is available on the metamorphosis of the mouth area in any euthyneuran with a planktotrophic larval stage.

Homology of the buccal pump

Our data suggest that the first part of the buccal pump (buccal pump 1) in adults of *O. tenuisculpta* is a transformation of a portion of the dorsal module, specifically, a part of the larval esophagus. Ultrastructural observations on animals sectioned at one day after velum loss were critical to this interpretation. At this stage, discoidal reticulate lamellae, which are diagnostic esophageal features of gastropod larvae (Bonar and Maugel, 1982), were still present at the apical surface of epithelial cells forming the developing buccal pump 1. Even before metamorphosis, condensations of cells accumulated around this area of the larval esophagus, which is not typical of foregut development in other gastropods with planktotrophic larvae. These cells differentiated after metamorphosis as the multiple layers of muscle investing the internal epithelial wall of buccal pump 1.

Buccal pump 2 was also clearly recognizable at four days after velum loss, although not completely differentiated at this time. We can only assume that buccal pump 2 was added as an extension of buccal pump 1. Unfortunately, we did not fix animals for sectioning between one and four days after the onset of metamorphosis, which was the critical time interval for initial formation of this second part of the buccal pump.

Oral tube

An oral tube dorsal to the stylet complex is present in pyramidellids in the genera *Odostomia*, *Boonea*, and *Sayella* (Maas, 1965; Wise, 1993, 1996; Hori and Okutani, 1995, 1996; Peterson, 1998). It is an epithelial tube running parallel and dorsal to the stylet complex between the sucker and the buccal pump. Our results for *O. tenuisculpta* suggested that this tube was not a portion of retained larval esophagus, because larval esophageal tissue above the buccal sac at one day after velum loss had completely dissociated. At this time, the future buccal sac had an undivided lumen. By four days after velum loss, the lumen of the buccal sac had become subdivided into the oral tube and the blind-ending dorsal cavity of the stylet complex. This segregation was likely effected by remodeling of the epithelial lining of the buccal sac, specifically, fusion of buccal sac epithelium along a horizontal plane running longitudinally down the buccal sac. We speculate that this process of epithelial remodeling does not occur in pyramidellids that lack a distinct oral tube. The oral tube of *O. tenuisculpta*, formed by longitudinal subdivision of the lumen of the buccal sac, appears to be a unique structure that is not obviously homologous to anything described to date in non-pyramidellid gastropods.

Foregut modularity and ontogenetic conflict

Based on other studies of foregut development in marine gastropods with a feeding larval stage, we expected to see extensive development of adult foregut structures in late-stage larvae of *O. tenuisculpta* (D'Asaro, 1965; Fretter, 1969; Thiriot-Quiévreux, 1970; Bickell and Chia, 1979; Page and Pedersen, 1998; Page, 2002, 2005; Parries and Page, 2003). Our hypothesis predicted that the modular developmental organization of the gastropod foregut, including that of *O. tenuisculpta*, would facilitate this without compromising feeding by larvae on microalgae. In reality, however, with the exception of the introvert tube and the salivary glands and their ducts, differentiation of juvenile foregut structures in larvae of *O. tenuisculpta* progressed only to the stage of generating non-differentiated precursor cells.

Foregut development in *O. tenuisculpta* is a case where the need for speed hypothesis, defined by Hadfield and coworkers (Hadfield, 2000; Hadfield *et al.*, 2001) as extensive development of juvenile structures in larvae to facilitate rapid metamorphosis, comes into major conflict with the larval constraint hypothesis, defined by Fretter (1969) as the need to maintain the functional integrity of larval structures until metamorphosis. In *O. tenuisculpta*, larval constraint has prevailed to a much greater extent than in other gastropods studied to date. As a result, metamorphosis involved not only loss of larval-specific structures but also a great deal of new morphogenesis. Juveniles of *O. tenuisculpta* did not begin feeding until 10 days after onset of metamorphosis, whereas other gastropods reared through larval and metamorphic stages at a similar temperature and obtained from source populations living in Pacific waters around the southern coast of Vancouver Island required a much shorter time period for metamorphosis. For example, *Trichotropis cancellata* began feeding at

several hours to several days (Parries and Page, 2003) and *Nassarius mendicus* began post-metamorphic feeding at three to five days after loss of the velar lobes (Page, 2005).

We suggest that many of the differentiated cells and cellular secretion products of the functioning post-metamorphic foregut in pyramidellids such as *O. tenuisculpta* cannot coexist with a functioning larval foregut. When juveniles of *O. tenuisculpta* began feeding after metamorphosis, the dagger-like stylet complex measured one-third the length of the shell. This structure is likely incompatible with maintaining a functional larval esophagus. Similarly, the tissue architecture of the buccal pump, with its chitin-lined lumen and muscular wall, is radically different than the simple, ciliated epithelium of the larval esophagus.

The process of foregut metamorphosis in *O. tenuisculpta* was unorthodox not only because of the many components that do not commence cellular differentiation until after metamorphosis is triggered but also because metamorphosis involved extensive elaboration of a dorsal module component, specifically, the buccal pump. Previous studies of foregut development in caenogastropods with a feeding larval stage have shown that the dorsal module begins as the larval esophagus. This module becomes remodeled at metamorphosis, mainly through loss of some of its cells, but it continues to function as part of the ciliated channel for food transport after metamorphosis (Page and Hookham, 2017). However, in *O. tenuisculpta*, a segment of larval esophagus (dorsal module) becomes hugely modified as buccal pump 1 and possibly also buccal pump 2. Post-metamorphic elaboration of dorsal module areas of the foregut may be more common in euthyneurans than currently appreciated.

It has been previously proposed that the modular organization for the developing foregut of gastropods may have facilitated the adaptive radiation of proboscis-bearing buccinoid and muricoid neogastropods because the ventral module, which forms most of the structures that will be used for post-metamorphic feeding, has become physically separated from the dorsal module, which forms the larval esophagus. Consequently, phenotypic variants of ventral module components could arise during development and be tested within the post-metamorphic environment without having to first pass through the "filter" of compatibility with the larval feeding system. Surprisingly, however, while dorsal and ventral foregut modules were recognizable during development of the pyramidellid *O. tenuisculpta*, the two modules did not show spatial uncoupling during larval development. Instead, we found evidence of temporal uncoupling of components within the ventral module, suggesting a loss of integration. Some components of the ventral module, notably the salivary glands, achieved advanced differentiation prior to larval metamorphosis; but secretion of the stylet complex was delayed until after the onset of metamorphosis. Furthermore, morphogenesis of a novel dorsal module component, the buccal pump, did not advance beyond provision of progenitor muscle cells prior to metamorphosis. We conclude that while subdivision of the gastropod foregut into two developmental modules and subsequent spatial uncoupling of these modules may have facilitated adaptive radiation within some gastropod lineages (Page and Hookham, 2017), modularity cannot explain evolution of the highly unusual feeding system of pyramidellids. This result adds to previous examples in which developmental modularity has not played a facilitating role during an adaptive radiation (Beldade *et al.*, 2002; Monteiro and Nogueira, 2010; Sanger *et al.*, 2012).

Acknowledgments

We thank Erick Jantzen for assistance with sectioning and Brent Gowen for assistance with electron microscopy. We also thank Rick M. Harbo for advice on collecting *Odostomia tenuisculpta*. A Discovery Grant from the Natural Sciences and Engineering Research Council of Canada supported this research and is gratefully acknowledged.

Literature Cited

Abbott, R. T. 1974. *American Seashells: The Marine Mollusca of the Atlantic and Pacific Coasts of North America*. 2nd ed. Van Nostrand Reinhold, New York.

Andersen, R. A., J. A. Berges, P. J. Harrison, and M. M. Watanabe. 2005. Appendix. Pp. 429–538 in *Algal Culturing Techniques*, R. A. Andersen, ed. Elsevier Academic, Burlington, MA.

Ankel, W. E. 1949a. Die Mundbewaffnung der Pyramidelliden. *Arch. Molluskenkd.* **77:** 79–82.

Ankel, W. E. 1949b. Die Nahrungsaufnahme der Pyramidelliden. *Ver. Dtsch. Zool.* **13(suppl. B):** 478–484.

Atchley, W. R., and B. K. Hall. 1991. A model for development and evolution of complex morphological structures. *Biol. Rev.* **66:** 101–157.

Beldade, P., K. Koops, and P. M. Brakefield. 2002. Modularity, individuality, and evo-devo in butterfly wings. *Proc. Natl. Acad. Sci. U.S.A.* **99:** 14262–14267.

Bickell, L. R., and F. S. Chia. 1979. Organogenesis and histogenesis in the planktotrophic veliger of *Doridella steinbergae* (Opisthobranchia: Nudibranchia). *Mar. Biol.* **52:** 291–313.

Bonar, D. B., and M. G. Hadfield. 1974. Metamorphosis of the marine gastropod, *Phestilla sibogae* Bergh (Nudibranchia: Aeolidacea). I. Light and electron microscopic analysis of larval and metamorphic stages. *J. Exp. Mar. Biol. Ecol.* **16:** 227–255.

Bonar, D. B., and T. K. Maugel. 1982. Particle exclusion by discoidal reticulate lamellae in larval gastropod feeding structures. *J. Ultrastruct. Res.* **81:** 88–103.

Cloney, R. A., and E. Florey. 1968. Ultrastructure of cephalopod chromatophore organs. *Z. Zellforsch.* **89:** 250–280.

Collin, R., and J. B. Wise. 1997. Morphology and development of *Odostomia columbiana* Dall and Bartsch (Pyramidellidae): implications for the evolution of gastropod development. *Biol. Bull.* **192:** 243–252.

Cumming, R. L. 1993. Reproduction and variable larval development of an ectoparasitic snail, *Turbonilla* sp. (Pyramidellidae, Opisthobranchia), on cultured giant clams. *Bull. Mar. Sci.* **52:** 760–771.

D'Asaro, C. N. 1965. Organogenesis, development, and metamorphosis in the queen conch, *Strombus gigas*, with notes on breeding habits. *Bull. Mar. Sci. Gulf Caribb.* **15:** 359–416.

Dinapoli, A., and A. Klussmann-Kolb. 2010. The long way to diversity: phylogeny and evolution of the Heterobranchia (Mollusca: Gastropoda). *Mol. Phylogenet. Evol.* **55:** 60–75.

Esteve-Altava, B. 2017. In search of morphological modules: a systematic review. *Biol. Rev.* **92:** 1332–1347.

Fiala, J. C. 2005. Reconstruct: a free editor for serial section microscopy. *J. Microsc.* **218:** 52–61.

Fretter, V. 1969. Aspects of metamorphosis in prosobranch gastropods. *Proc. Malacol. Soc. Lond.* **38:** 375–385.

Fretter, V., and A. Graham. 1949. The structure and mode of life of the Pyramidellidae, parasitic opisthobranchs. *J. Mar. Biol. Assoc. U.K.* **28:** 493–532.

Fretter, V., and A. Graham. 1962. *British Prosobranch Gastropods.* Ray Society, London.

Golding, R. E., W. F. Ponder, and M. Byrne. 2009. The evolutionary and biomechanical implications of snout and proboscis morphology in Caenogastropoda (Mollusca: Gastropoda). *J. Nat. Hist.* **43:** 2723–2763.

Hadfield, M. G. 2000. Why and how marine-invertebrate larvae metamorphose so fast. *Semin. Cell. Dev. Biol.* **11:** 437–443.

Hadfield, M. G., E. J. Carpizo-Ituarte, K. del Carmen, and B. T. Nedved. 2001. Metamorphic competence, a major adaptive convergence in marine invertebrate larvae. *Am. Zool.* **41:** 1123–1131.

Harbo, R., N. McDaniel, and P. Lafollette. 2012. An exciting new discovery: the lightly-sculpted odostome snail, *Evalea tenuisculpta* (Carpenter, 1864) feeding on the siphon tips of the fat gaper, *Tresus capax* (Gould, 1850) in Vancouver Harbour, British Columbia. *Dredgings* **52:** 3–4.

Hendrikse, J. L., T. E. Parsons, and B. Hallgrímsson. 2007. Evolvability as the proper focus of evolutionary developmental biology. *Evol. Dev.* **9:** 393–401.

Hirose, E. 2005. Digestive system of the sacoglossan *Plakobranchus ocellatus* (Gastropoda: Opisthobranchia): light- and electron-microscopic observations with remarks on chloroplast retention. *Zool. Sci.* **22:** 905–916.

Hori, S., and T. Okutani. 1995. A new pyramidellid gastropod ectoparasitic on *Umbonium* (*Suchium*) *moniliferum* (Lamarck) from Tomioka Bay, Amakusa, Western Kyushu. *Venus* **54:** 247–258.

Hori, S., and T. Okutani. 1996. A new pyramidellid gastropod ectoparasitic on *Conus*. *Venus* **55:** 7–14.

Howells, H. H. 1942. The structure and function of the alimentary canal of *Aplysia punctata*. *Q. J. Microsc. Sci.* **83:** 357–397.

Hughes, R. L. 1979. Ultrastructure of the buccal mass in juvenile *Coryphella salmonacea* (Gastropoda: Nudibranchia). *J. Molluscan Stud.* **45:** 289–295.

Hurst, A. 1967. The egg masses and veligers of thirty Northeast Pacific opisthobranchs. *Veliger* **9:** 255–288.

Jensen, K. E. 1993. Morphological adaptations and plasticity of radular teeth of the Sacoglossa (=Ascoglossa) (Mollusca: Opisthobranchia) in relation to their food plants. *Biol. J. Linn. Soc.* **48:** 135–155.

Kerth, K. 1979. Electron microscopic studies on radular tooth formation in the snails *Helix pomatia* L. and *Limax flavus* L. (Pulmonata, Stylommatophora). *Cell Tissue Res.* **203:** 283–289.

Kerth, K., and G. Krause. 1969. Untersuchungen mittels Röntgenbestrahlung über den Radula-Ersatz der Nacktschnecke *Limax flavus* L. *Wilhelm Roux Arch.* **164:** 48–82.

Klingenberg, C. P. 2008. Morphological integration and developmental modularity. *Annu. Rev. Ecol. Evol. Syst.* **39:** 115–132.

Maas, D. 1965. Anatomische und Histologische Untersuchungen am Mundapparat der Pyramidelliden. *Z. Morphol. Oekol. Tiere* **54:** 566–642.

Mackenstedt, U., and K. Märkel. 1987. Experimental and comparative morphology of radula renewal in pulmonates (Mollusca, Gastropoda). *Zoomorphology* **107:** 209–239.

Maguire, A. K., and L. Rogers-Bennett. 2013. An ectoparasitic snail (*Evalea tenuisculpta*) infects red abalone (*Haliotis rufescens*) in northern California. *Calif. Fish Game* **99:** 80–89.

Mikhlina, A., A. Tzetlin, and E. Vortsepneva. 2018. Renewal mechanisms of buccal armature in *Flabellina verrucosa* (Nudibranchia: Aeolidida: Flabellinidae). *Zoomorphology* **137:** 31–50.

Mischor, B., and K. Markel. 1984. Histology and regeneration of the radula of *Pomacea bridgesi* (Gastropoda, Prosobranchia). *Zoomorphology* **104:** 42–66.

Monteiro, L. R., and M. R. Nogueira. 2010. Adaptive radiations, ecological specialization, and the evolutionary integration of complex morphological structures. *Evolution* **64:** 724–744.

Page, L. R. 2000. Development and evolution of adult feeding structures in caenogastropods: overcoming larval functional constraints. *Evol. Dev.* **2:** 25–34.

Page, L. R. 2002. Larval and metamorphic development of the foregut and proboscis in the caenogastropod *Marsenina* (*Lamellaria*) *stearnsii*. *J. Morphol.* **252:** 202–217.

Page, L. R. 2005. Development of foregut and proboscis in the buccinid neogastropod *Nassarius mendicus*: evolutionary opportunity exploited by a developmental module. *J. Morphol.* **264:** 327–338.

Page, L. R. 2009. Molluscan larvae: pelagic juveniles or slowly metamorphosing larvae? *Biol. Bull.* **216:** 216–225.

Page, L. R., and B. Hookham. 2017. The gastropod foregut: evolution viewed through a developmental lens. *Can. J. Zool.* **95:** 227–238.

Page, L. R., and R. V. L. Pedersen. 1998. Transformation of phytoplanktivorous larvae into predatory carnivores during the development of *Polinices lewisii* (Mollusca, Caenogastropoda). *Invertebr. Biol.* **117:** 208–220.

Page, L. R., I. M. Hildebrand, and S. C. Kempf. 2019. Siphonariid development: quintessential euthyneuran larva with a mantle fold innovation (Gastropoda; Panpulmonata). *J. Morphol.* **280:** 634–653.

Parries, S. C., and L. R. Page. 2003. Larval development and metamorphic transformation of the feeding system in the kleptoparasitic snail *Trichotropis cancellata* (Mollusca, Caenogastropoda). *Can. J. Zool.* **81:** 1650–1661.

Peterson, B. J. 1998. The morphology, ultrastructure and function of the feeding apparatus of *Sayella fusca* (C.B. Adams, 1839) (Gastropoda: Pyramidellidae). *J. Molluscan Stud.* **64:** 281–296.

Ponder, W. F. 1973. The origin and evolution of the Neogastropoda. *Malacologia* **12:** 295–338.

Raff, R. A. 1996. *The Shape of Life: Genes, Development, and the Evolution of Animal Form*. University of Chicago Press, Chicago.

Raff, R. A. 2000. Evo-devo: the evolution of a new discipline. *Nat. Rev. Genet.* **1:** 74–79.

Richardson, K. C., L. Jarrett, and E. H. Finke. 1960. Embedding in epoxy resins for ultrathin sectioning in electron microscopy. *Stain Technol.* **35:** 313–323.

Robertson, R. 2012. Pyramidellid protoconchs, eggs, embryos and larval ecology: an introductory survey. *Am. Malacol. Bull.* **30:** 219–228.

Robertson, R., and T. Mau-Lastovicka. 1979. The ectoparasitism of *Boonea* and *Fargoa* (Gastropoda: Pyramidellidae). *Biol. Bull.* **157:** 320–333.

Rudman, W. B. 1972. The anatomy of the opisthobraanch genus *Hydatina* and the functioning of the mantle cavity and alimentary canal. *Zool. J. Linn. Soc.* **51:** 121–139.

Runham, N. W. 1975. Alimentary canal. Pp. 53–104 in *Pulmonates*, Vol. I, V. Fretter and J. Peake, eds. Academic Press, New York.

Sanger, T. J., D. L. Mahler, A. Abzhanov, and J. B. Losos. 2012. Roles for modularity and constraint in the evolution of cranial diversity among *Anolis* lizards. *Evolution* **66:** 1525–1542.

Schander, C., S. Hori, and J. Lundberg. 1999. Anatomy, phylogeny and biology of *Odostomella* and *Herviera*, with the description of a new species of *Odostomella* (Mollusca, Heterostropha, Pyramidellidae). *Ophelia* **51:** 39–76.

Schander, C., K. M. Halanych, T. Dahlgren, and P. Sundberg. 2003. Test of the monophyly of Odostomiinae and Turbonilliinae (Gastropoda, Heterobranchia, Pyramidellidae) based on 16S mtDNA sequences. *Zool. Scr.* **32:** 243–254.

Schlosser, G., and G. P. Wagner. 2004. *Modularity in Development and Evolution*. University of Chicago Press, Chicago.

Shaw, J. A., D. J. Macey, L. R. Brooker, E. J. Stockdale, M. Saunders, and P. L. Clode. 2009. Ultrastructure of the epithelial cells associated with tooth biomineralization in the chiton *Acanthopleura hirtosa*. *Microsc. Microanal.* **15:** 154–165.

Simone, L. R. L. 2011. Phylogeny of the Caenogastropoda (Mollusca) based on comparative morphology. *Arq. Zool.* **42:** 161–323.

Strong, E. E. 2003. Refining molluscan characters: morphology, character coding and a phylogeny of the Caenogastropoda. *Zool. J. Linn. Soc.* **137:** 447–554.

Switzer-Dunlap, M., and M. G. Hadfield. 1977. Observations on development, larval growth and metamorphosis of four species of Aplysiidae (Gastropoda: Opisthobranchia) in laboratory culture. *J. Exp. Mar. Biol. Ecol.* **29:** 245–261.

Taylor, J. D., N. J. Morris, and C. N. Taylor. 1980. Food specialization and the evolution of predatory prosobranch gastropods. *Palaeontology* **23:** 375–409.

Thiriot-Quiévreux, C. 1970. Transformations histologiques lors de la métamorphose cheq *Cymbulia peroni* de Blainville (Mollusca, Opisthobranchia). *Z. Morphol. Tiere* **67:** 106–117.

Vortsepneva, E. V., and A. B. Tzetlin. 2014. New data on the fine structure of hooks in *Clione limacina* (Gastropoda, Opisthobranchia) and diversity of the jaw apparatus in gastropods. *Zool. Zh.* **93:** 466–478.

Wagner, G. P., and L. Altenberg. 1996. Perspective: complex adaptations and the evolution of evolvability. *Evolution* **50:** 967–976.

Wagner, G. P., M. Pavlicev, and J. M. Cheverud. 2007. The road to modularity. *Nat. Rev. Genet.* **8:** 921–931.

White, M. E., C. L. Kitting, and E. N. Powell. 1985. Aspects of reproduction, larval development, and morphometrics in the pyramidellid *Boonea impressa* (=*Odostomia impressa*) (Gastropoda: Opisthobranchia). *Veliger* **28:** 37–51.

Wiesel, R., and W. Peters. 1978. Licht- und elektronenmikroskopische Untersuchungen am Radulakomplex und zur Radulabildung von *Biomphalaria glabrata* Say (=*Australorbis gl*) (Gastropoda, Basommatophora). *Zoomorphologie* **89:** 73–92.

Wise, J. B. 1993. Anatomy and functional morphology of the feeding structures of the ectoparasitic gastropod *Boonea impressa* (Pyramidellidae). *Malacologia* **35:** 119–134.

Wise, J. B. 1996. Morphology and phylogenetic relationships of certain pyramidellid taxa (Heterobranchia). *Malacologia* **37:** 443–511.

Zapata, F., N. G. Wilson, M. Howison, S. C. S. Andrade, K. M. Jörger, M. Schrödl, F. E. Goetz, G. Giribet, and C. W. Dunn. 2014. Phylogenomic analyses of deep gastropod relationships reject Orthogastropoda. *Proc. R. Soc. B Biol. Sci.* **281:** 20141739.